arXiv:1202.4879v1 [physics.ao-ph] 22 Feb 2012

Angular distribution of Bremsstrahlung photons and of positrons for calculations of terrestrial gamma-ray flashes and positron beams

Christoph Köhn[a] and Ute Ebert[a,b]

[a] *CWI, P.O.Box 94079, 1090GB Amsterdam, The Netherlands, and*
[b] *Eindhoven University of Technology, P.O.Box 513, 5600MB Eindhoven, The Netherlands.*

Abstract

Within thunderstorms electrons can gain energies of up to hundred(s) of MeV. These electrons can create X-rays and gamma-rays as Bremsstrahlung when they collide with air molecules. Here we calculate the distribution of angles between incident electrons and emitted photons as a function of electron and photon energy. We derive these doubly differential cross-sections by integrating analytically over the triply differential cross-sections derived by Bethe and Heitler; this is appropriate for light atoms like nitrogen and oxygen and for electron energies between 1 keV and 1 GeV. We also discuss some simplifying limit cases, and we derive some simple approximation for the most probable scattering angle.

We also provide cross sections for the production of electron positron pairs from energetic photons when they interact with air molecules. This process is related to the Bremsstrahlung process by some physical symmetry. Therefore the results above can be transferred to predictions on the angles between incident photon and emitted positron, again as a function of photon and positron energy. We present the distribution of angles and again a simple approximation for the most probable scattering angle.

Our results are given as analytical expressions as well as in the form of a C++ code that can be directly be implemented into Monte Carlo codes.

Keywords: Bremsstrahlung, pair production, analytical integration of Bethe-Heitler equation, distribution of scattering angles

---

Email address: `koehn@cwi.nl`, `ebert@cwi.nl` (Christoph Köhn[a] and Ute Ebert[a,b])

Preprint submitted to Elsevier *February 23, 2012*

---

1. Introduction

1.1. Flashes of gamma-rays, electrons and positrons above thunderclouds

Terrestrial gamma ray flashes (TGFs) were first observed above thunderclouds by the Burst and Transient Source Experiment (BATSE) (Fishman et al., 1994). It was soon understood that these energetic photons were generated by the Bremsstrahlung process when energetic electrons collide with air molecules (Fishman et al., 1994; Torii et al., 2004); these electrons were accelerated by some mechanism within the thunderstorm. Since then, measurements of TGF's were extended and largely refined by the Reuven Ramaty Energy Solar Spectroscopic Imager (RHESSI) (Cummer et al., 2005; Smith et al., 2005, Grefenstette et al., 2009, Smith et al., 2010; Lu et al., 2011), by the Fermi Gamma-ray Space Telescope (Briggs et al., 2010), by the Astrorivelatore Gamma a Immagini Leggero (AGILE) satellite which recently measured TGFs with quantum energies of up to 100 MeV (Marisaldi et al., 2010; Smith et al., 2011; Tavani et al., 2011), and by the Gamma-Ray Observation of Winter Thunderclouds (GROWTH) experiment (Tsuchiya et al., 2011).

Hard radiation was also measured from approaching lightning leaders (Moore et al., 2001; Dwyer et al., 2005); and there are also a number of laboratory experiments where very energetic photons were generated during the streamer-leader stage of discharges in open air (Stankevich and Kalinin, 1967; Dwyer et al., 2005b; Kostyrya et al., 2006; Dwyer et al., 2008b; Nguyen et al., 2008; Rahmen et al., 2008; Rep'ev and Repin, 2008; Nguyen et al., 2010; March and Montanyà, 2010; Shao et al., 2011).

Next to gamma-ray flashes, flashes of energetic electrons have been detected above thunderstorms (Dwyer et al., 2008b); they are distinguished from gamma-ray flashes by their dispersion and their location relative to the cloud - as charged particles in sufficiently thin air follow the geomagnetic field lines. In December 2009 NASA's Fermi satellite detected a substantial amount of positrons within these electron beams (Briggs et al., 2011). It is now generally assumed that these positrons come from electron positron pairs that are generated when gamma-rays collide with air molecules.

Two different mechanisms for creating large amounts of energetic electrons in thunderclouds are presently discussed in the literature. The older suggestion is a relativistic run-away process in a rather homogeneous electric field inside the cloud (Wilson, 1925; Gurevich, 1961; Gurevich et al., 1992; Gurevich, 2001 Dwyer, 2003, 2007; Milikh and Roussel-Dupré, 2010).

More recently research focusses on electron acceleration in the streamer-leader process with its strong local field enhancement (Moss et al., 2006; Li et al., 2007; Chanrion and Neubert, 2008; Li et al., 2009; Carlson et al., 2010; Celestin and Pasko, 2011; Li et al., 2012).

1.2. The need for doubly differential cross-sections

Whatever the mechanism of electron acceleration in thunderstorms is, ultimately one needs to calculate the energy spectrum and angular distribution of the emitted Bremsstrahlung photons. As the electrons at the source form a rather directed beam pointing against the direction of the local field, the electron energy distribution together with the angles and energies of the emitted photons determine the photon energy spectrum measured by some remote detector. The energy resolved photon scattering angles are determined by so-called doubly differential cross-sections that resolve simultaneously energy $\hbar\omega$ and scattering angle Θ_i of the photons for given energy E_i of the incident electrons. The data is required for scattering on the light elements nitrogen and oxygen with atomic numbers $Z = 7$ and $Z = 8$, while much research in the past has focussed on metals with large atomic numbers Z. The energy range up to 1 GeV is relevant for TGF's; we here will provide data valid for energies above 1 keV.

As illustrated by Fig. 1, the full scattering problem is characterized by three angles. The two additional angles Θ_f and Φ determine the direction of the scattered electron relative to the incident electron and the emitted photon. The full angular and energy dependence of this process is determined by so-called triply differential cross-sections. A main result of the present paper is the analytical integration over the angles Θ_f and Φ to determine the doubly differential cross-sections relevant for TGF's.

As the cross-sections for the production of electron positron pairs from photons in the field of some nucleus are related by some physical symmetry to the Bremsstrahlung process, we study these processes as well; we provide doubly differential cross-sections for scattering angle Θ_+ and energy E_+ of the emitted positrons for given incident photon energy $\hbar\omega$ and atomic number Z.

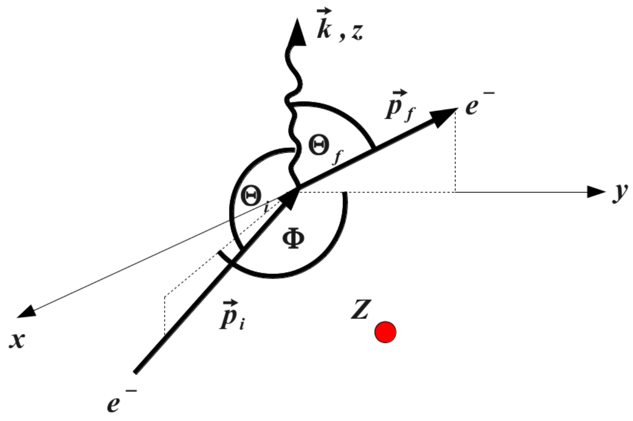

Figure 1: Parametrization of the Bremsstrahlung process: Momenta of incident electron $\mathbf{p}_i$, scattered electron $\mathbf{p}_f$ and emitted photon $\hbar\mathbf{k}$ form the angles $\Theta_i = \sphericalangle(\mathbf{p}_i, \mathbf{k})$ and $\Theta_f = \sphericalangle(\mathbf{p}_f, \mathbf{k})$, and Φ is the angle between the planes spanned by the vector pairs $(\mathbf{p}_i, \mathbf{k})$ and $(\mathbf{p}_f, \mathbf{k})$. The scattering nucleus has atomic number Z.

1.3. Available cross-sections for Bremsstrahlung

Our present understanding of Bremsstrahlung and pair production was largely developed in the first half of the 20th century. It was first calculated by Bethe and Heitler (1934). Important older reviews are by Heitler (1944), by Hough (1948), and by Koch and Motz (1959). We also used some recent text books (Greiner and Reinhardt, 1995; Peskin and Schroeder, 1995); together with Heitler (1944) and Hough (1948), they provide a good introduction into the quantum field theoretical description of Bremsstrahlung and pair production. The calculation of these two processes is related through some physical symmetry as will be explained in chapter 3.

As drawn in Fig. 1, when an electron scatters at a nucleus, a photon with frequency ω can be emitted. The geometry of this process is described by the three angles Θ_i, Θ_f and Φ. Cross sections can be total or differential. Total cross sections determine whether a collision takes place for given incident electron energy, singly differential cross sections give additional information on the photon energy or on the angle between incident electron and emitted photon, and doubly differential cross sections contain both. Triply differential cross sections additionally contain the angle at which the electron is scattered. As two angles are required to characterize the direction of the scattered electron, one could argue that this cross section should actually be called quadruply differential, but the standard terminology for the process is triply differential.

Koch and Motz (1959) review many different expressions for different limiting cases, but without derivations. Moreover, some experimental results are discussed and compared with the presented theory. Bethe and Heitler (1934), Heitler (1944), Hough (1948), Koch and Motz (1959), Peskin and Schroeder (1995), Greiner and Reinhardt (1955) use the Born approximation to derive and describe Bremsstrahlung and pair production cross sections.

Several years later new ansatzes were made to describe Bremsstrahlung. Elwert and Haug (1969) use approximate Sommerfeld-Maue eigenfunctions to derive cross sections for Bremsstrahlung under the assumption of a pure Coulomb field. They derive a triply differential cross section and beyond that also numerically a doubly differential cross section. Furthermore they compare with results obtained by using the Born approximation. They show that there is a small discrepancy for high atomic numbers between the Bethe-Heitler theory and experimental data, and they provide a correcting factor to fit the Bethe-Heitler approximation better to experimental data for large Z. However, they only investigate properties of Bremsstrahlung for $Z = 13$ (aluminum) and $Z = 79$ (gold).

Tseng and Pratt (1971) and Fink and Pratt (1973) use exact numerical calculations using Coulomb screened potentials and Furry-Sommerfeld-Maue wave functions, respectively. They investigate Bremsstrahlung and pair production for $Z = 13$ and for $Z = 79$ and show that their results with more accurate wave functions do not fit with the Bethe Heitler cross section exactly. This is not surprising as the Bethe-Heitler approximation is developed for low atomic numbers Z and for Z dependent electron energies as discussed in section 2.2.

Shaffer et al. (1996) review the Bethe Heitler and the Elwert Haug theory. They discuss that the Bethe Heitler approach is good for small atomic numbers and give a limit of $Z > 29$ for experiments to deviate from theory. They calculate triply differential cross sections using partial-wave and multipole expansions in a screened potential numerically for $Z = 47$ (silver) and $Z = 79$ and compare their results with experimental data. Actually their results are close to the Elwert Haug theory which fits the experimental data better than their theory.

Shaffer and Pratt (1997) also discuss the theory of Elwert and Haug (1969) and compare it with the Bethe Heitler theory and, additionally, with the Bethe Heitler results multiplied with the Elwert factor and with the exact partial wave method. They show that all theories agree within a factor 10 in the keV energy range, and that the Elwert-Haug theory fits the exact partial wave method best. However, they only investigate Bremsstrahlung for atomic nuclei with $Z = 47$, 53 (iodine), 60 (neodymium), 68 (erbium) and 79, but not for small atomic numbers $Z = 7$ and 8 as relevant in air. In summary, Elwert and Haug (1969), Tseng and Pratt (1971), Fink and Pratt (1973), Shaffer et al. (1996) and Shaffer and Pratt (1997) calculate cross sections for Bremsstrahlung and pair production for atomic numbers $Z = 13$ and $Z > 47$ numerically, but not analytically, and they do not provide any formula or data which can be used to simulate discharges in air.

The EEDL database consists mainly of experimental data which have been adjusted to nuclear model calculations. For the low energy range Geant4 takes over this data and gives a fit formula. The singly differential cross section related to ω which is used in the Geant4 database is valid in an energy range from 1 keV to 10 GeV and taken from Seltzer and Berger (1985). The singly differential cross section related to Θ_i is based on the doubly differential cross section by (Tsai, 1974; Tsai, 1977) and valid for very high energies, i.e., well above $(1-10)$ MeV. But in the Geant4 database the dependence on the photon energy is neglected in this case so that it is actually a singly differential cross section describing Θ_i.

Table 1 gives an overview of the available literature and data for total or singly, doubly or triply differential Bremsstrahlung cross sections; parameterized angles or photon energies are given, as well as the different energy ranges of the incident electron. Furthermore, the table shows the atomic number Z investigated and includes some further remarks.

For calculating the angularly resolved photon energy spectrum of TGF's, we need a doubly differential cross section resolving both energy and emission angle of the photons; we need it in the energy range between 1 keV and 1 GeV for the small atomic numbers $Z = 7$ and 8. Therefore most of the literature reviewed here is not applicable. However, the Bethe-Heitler approximation is valid for atomic numbers $Z < 29$ and for electron energies above 1 keV (Shaffer et al., 1996). How the range of validity depends on the atomic number Z is discussed in section 2.2. We therefore will use the triply differential cross section derived by Bethe and Heitler (1934) to determine the correct doubly differential cross.

Data/Paper	Information	Energy range	Atomic Number Z	Remarks
Bethe and Heitler (1934,1944)	ω $\omega, \Theta_i, \Theta_f, \Phi$	1 keV - 1 GeV	7,8	energy range depends on Z
Koch and Motz (1959)	Total ω ω, Θ_i, Φ $\omega, \Theta_i, \Theta_f, \Phi$	different lower bounds, no upper bounds	depends on the used formulae	
Aiginger (1966)	ω, Θ_i	180, 380 keV	79, Al_2O_3	experimental
Elwert and Haug (1969)	ω, Θ_i $\omega, \Theta_i, \Theta_f, \Phi$	keV range	13,79	
Penczynski and Wehner (1970)	ω, Θ_i	(300 ± 10) keV	82	experimental
Tseng and Pratt (1971)	$\omega, \Theta_i, \Theta_f, \Phi$	keV, MeV range	13,79	
Fink and Pratt (1973)	ω $\omega, \Theta_i, \Theta_f, \Phi$	keV, MeV range	6,13,79,92	also for pair production
Tsai (1974,1977)	ω, Θ_i	$>$ few 10 MeV	all	
Seltzer and Berger (1985)	ω	1 keV - 10 GeV	Z=6,13,29,47,74,92	
EEDL (1991)	Total	5 eV - 1 TeV	all	see (Cullen et al., 1991)
Nackel (1994)	ω, Θ_i	keV	6,29,47,79	only twodimensional description
Schaffer et al. (1996)	ω, Θ_i, Φ	keV range	6,13,29,47,74,92	
Schaffer and Pratt (1997)	$\omega, \Theta_i, \Theta_f, \Phi$ ω, Θ_i	keV range	47,53,60,68,79	
Lehtinen (2000)	ω, Θ_i	1 keV - 1 GeV	7,8	Simple product ansatz for angular and frequency part
Geant 4 (2003)	Total ω Θ_i	5 eV - 1 TeV 1 keV - 10 GeV $>$ few 10 MeV	all 6,13,29,47,74,92 all	based on EEDL based on Seltzer and Berger (1985) based on Tsai (1974, 1977)

Table 1: Available data for Bremsstrahlung cross sections. Besides the available information on total or singly, doubly or triply differential cross-sections, the range of validity of the incident electron energy and of the atomic number is given. If not stated otherwise, these are theoretical expressions.

I

1.4. Bremsstrahlung data used by other TGF researchers

Carlson et al. (2009, 2010) use the Geant 4 database to simulate the production of Terrestrial Gamma-Ray Flashes. But Geant 4 does not supply an energy resolved angular distribution as it does not contain a doubly differential cross section, parameterizing both energy and emission angle of the Bremsstrahlung photons (see Table 1). We will compare the Bethe-Heitler approximation with Geant 4 in Appendix D.

Lehtinen has suggested a doubly differential cross section in his PhD thesis (Lehtlinen, 2000) that is also used in a recently submitted manuscript by Celestin and Pasko. Lehtinen's ansatz is a heuristic approach based on factorization into two factors. The first factor is the singly differential cross section of Bethe and Heitler (1934) that resolves only electron and photon energies, but no angles. The second factor is due to Jackson (1975), it depends on the variable $(1-\beta^2)\ [(1-\beta\cos\Theta_i)^2+(\cos\Theta_i-\beta)]\ /\ (1-\beta\cos\Theta_i)^4$, where $\beta = |v_i|/c$ measures the incident electron velocity on the relativistic scale. However, this factor is derived in Jackson (1975) only in the relativistic case, e.g., for incident electron energies above 500 keV. Furthermore, the calculation is classical and not quantum mechanical, and it is valid only if the photon energy is much smaller than the total energy of the incident electron. We will compare this ansatz with our results in Appendix E.

Dwyer (2007) chooses to use the triply differential cross section by Bethe and Heitler (1934), but with an additional form factor parameterizing the structure of the nucleus (Koch and Motz, 1959). This cross section depends on all three angles as shown in Fig. 1. If one is only interested in the angle Θ_i between incident electron and emitted Bremsstrahlung photon, the angles Θ_f and Φ have to be integrated out — either numerically, or the analytical results derived in the present paper can be used.

1.5. Organization of the paper

In chapter 2 we introduce the triply differential cross section derived by Bethe and Heitler Then we integrate over the two angles Θ_f and Φ to obtain the doubly differential cross section which gives a correlation between the energy of the emitted photon and its direction relative to the incident electron. Furthermore, we investigate the limit of very small or very large angles and of high photon energies; this also serves as a consistency check for the correct integration of the full expression.

In chapter 3 we perform the same calculations for pair production, i.e., when an incident photon interacts with an atomic nucleus and creates a positron electron pair. As we explain, this process is actually related by some physical symmetry to Bremsstrahlung, therefore results can be transferred from Bremsstrahlung to pair production. We get a doubly differential cross section for energy and emission angle of the created positron relative to direction and energy of the incident photon.

The physical interpretation and implications of our analytical results is discussed in chapter 4. Energies and emission angles of the created photons and positrons are described in the particular case of scattering on nitrogen nuclei. For electron energies below 100 keV, the emission of Bremsstrahlung photons in different directions varies typically by not more than an order of magnitude, while for higher electron energies the photons are mainly emitted in forward direction. For this case, we derive an analytical approximation for the most likely emission angle of Bremsstrahlung photons and positrons for given particle energies.

In chapter 5 we will briefly summarize the results of our calculations.

Details of our calculations can be found in Appendix A - Appendix H. Beyond that we provide a C++ code in Appendix I which can be used to create data tables of our analytical results for doubly differential cross-sections both for Bremsstrahlung photons and for pair production positrons for use in Monte Carlo codes. The C++ code can also be directly downloaded from the website of the journal.

2. Bremsstrahlung

2.1. Definition of the process

If an electron with momentum $\mathbf{p}_i$ approaches the nucleus of an atom, it can change its direction due to Coulomb interaction with the nucleus; the electron acceleration creates a Bremsstrahlung photon with momentum $\mathbf{k}$ that can be emitted at an angle Θ_i relative to the initial direction of the electron. The new direction of the electron forms an angle Θ_f with the direction of the photon. The angle Φ is the angle between the planes spanned by the vector pairs $(\mathbf{p}_i, \mathbf{k})$ and $(\mathbf{p}_f, \mathbf{k})$. This process is shown in figure 1. A virtual photon (allowed by Heisenberg's uncertainty principle) transfers a momentum $\mathbf{q}$ between the electron and the nucleus. Therefore both energy and momentum are conserved in the scattering process.

The corresponding triply differential cross section was derived by Bethe and Heitler (1934):

$$\begin{aligned}
d^4\sigma &= \frac{Z^2\alpha_{fine}^3 h^2}{(2\pi)^2}\frac{|\mathbf{p}_f|}{|\mathbf{p}_i|}\frac{d\omega}{\omega}\frac{d\Omega_i d\Omega_f d\Phi}{|\mathbf{q}|^4}\times \\
&\times \Bigg[\frac{\mathbf{p}_f^2\sin^2\Theta_f}{(E_f - c|\mathbf{p}_f|\cos\Theta_f)^2}\left(4E_i^2 - c^2\mathbf{q}^2\right) \\
&+ \frac{\mathbf{p}_i^2\sin^2\Theta_i}{(E_i - c|\mathbf{p}_i|\cos\Theta_i)^2}\left(4E_f^2 - c^2\mathbf{q}^2\right) \\
&+ 2\hbar^2\omega^2\frac{\mathbf{p}_i^2\sin^2\Theta_i + \mathbf{p}_f^2\sin^2\Theta_f}{(E_f - c|\mathbf{p}_f|\cos\Theta_f)(E_i - c|\mathbf{p}_i|\cos\Theta_i)} \\
&- 2\,\frac{|\mathbf{p}_i||\mathbf{p}_f|\sin\Theta_i\sin\Theta_f\cos\Phi}{(E_f - c|\mathbf{p}_f|\cos\Theta_f)(E_i - c|\mathbf{p}_i|\cos\Theta_i)}\left(2E_i^2 + 2E_f^2 - c^2\mathbf{q}^2\right)\Bigg]. \qquad (1)
\end{aligned}$$

Here Z is the atomic number of the nulceus, $\alpha_{fine} \approx 1/137$ is the fine structure constant, $h \approx 6.63{\cdot}10^{-34}$ Js is Planck's constant, $\hbar = h/2\pi$ and $c \approx 3{\cdot}10^8$ m/s is the speed of light. The kinetic energy $E_{kin,i/f}$ of the electron in the initial and final state is related to its total energy and momentum as

$$E_{i/f} = E_{kin,i/f} + m_e c^2 = \sqrt{m_e^2 c^4 + \mathbf{p}_{i/f}^2 c^2} \qquad (2)$$

where $m_e \approx 9.1 \cdot 10^{-31}$ kg is the electron mass. The conservation of energy implies

$$E_f = E_i - \hbar\omega \qquad (3)$$

which determines E_f as a function of E_i and $\hbar\omega$. The directions of the emitted photon with energy $\hbar\omega$ and of the scattered electron are parameterized by the three angles (see Fig. 1)

$$\begin{aligned}\Theta_i &= \sphericalangle(\mathbf{p}_i, \mathbf{k}), & (4)\\ \Theta_f &= \sphericalangle(\mathbf{p}_f, \mathbf{k}), & (5)\\ \Phi &= \text{Angle between the planes } (\mathbf{p}_i, \mathbf{k}) \text{ and } (\mathbf{p}_f, \mathbf{k}). & (6)\end{aligned}$$

The differentials are

$$\begin{aligned}d\Omega_i &= \sin\Theta_i \; d\Theta_i, & (7)\\ d\Omega_f &= \sin\Theta_f \; d\Theta_f. & (8)\end{aligned}$$

Furthermore one can get an expression for the absolute value of the virtual photon $\mathbf{q}$ with the help of the momenta, the photon energy $\hbar\omega$ and the angles (4) - (6). Its value is

$$\begin{aligned}-\mathbf{q}^2 &= -|\mathbf{p}_i|^2 - |\mathbf{p}_f|^2 - \left(\frac{\hbar}{c}\omega\right)^2 + 2|\mathbf{p}_i|\frac{\hbar}{c}\omega\cos\Theta_i - 2|\mathbf{p}_f|\frac{\hbar}{c}\omega\cos\Theta_f \\ &+ 2|\mathbf{p}_i||\mathbf{p}_f|(\cos\Theta_f\cos\Theta_i + \sin\Theta_f\sin\Theta_i\cos\Phi). \qquad (9)\end{aligned}$$

2.2. Validity of the cross sections of Bethe and Heitler

The cross sections of Bethe and Heitler (1) are valid if the Born approximation (Bethe and Heitler, 1934) holds

$$v \gg \frac{Zc}{137} \qquad (10)$$

For nitrogen with $Z = 7$ and for oxygen with $Z = 8$, this holds for electron velocities $|\mathbf{v}_{Z=7}| \gg 15 \cdot 10^6$ m/s and $|\mathbf{v}_{Z=8}| \gg 18 \cdot 10^6$ m/s; this is equivalent to a kinetic energy of

$$E_{kin} = \frac{m_e c^2}{\sqrt{1 - \frac{v^2}{c^2}}} - m_e c^2 \gg \left\{ \begin{array}{l} 670 \text{ eV}, \; Z = 7 \\ 875 \text{ eV}, \; Z = 8 \end{array} \right. . \qquad (11)$$

This means that incident electron energies above 1 keV can be treated with Eq. 1, for lower energies, one cannot calculate with free electron waves anymore, but has to use Coulomb waves (Heitler, 1944; Greiner und Reinhardt, 1995); in this case one cannot derive cross sections like (1) analytically any more.

2.3. Integration over Φ

The easiest way is to integrate over the angle Φ between the scattering planes first (see Fig. 1) . For this purpose it is useful to redefine some quantities in the following way; therefore (1) can be written much more simply:

$$\begin{aligned}
\alpha &:= 2|\mathbf{p}_i||\mathbf{p}_f|\sin\Theta_i\sin\Theta_f, && (12)\\
\beta &:= -\mathbf{p}_i^2-\mathbf{p}_f^2-\left(\frac{\hbar}{c}\omega\right)^2-2\frac{\hbar}{c}\omega|\mathbf{p}_f|\cos\Theta_f+2\frac{\hbar}{c}\omega|\mathbf{p}_i|\cos\Theta_i \\
&+ 2|\mathbf{p}_i||\mathbf{p}_f|\cos\Theta_i\cos\Theta_f && (13)\\
A &:= \frac{Z^2\alpha_{fine}^3}{(2\pi)^2}\frac{|\mathbf{p}_f|}{|\mathbf{p}_i|}\frac{h^2}{\omega}, && (14)\\
a_1 &:= \left(\frac{|\mathbf{p}_f|^2c^2\sin^2\Theta_f}{(E_f-|\mathbf{p}_f|c\cos\Theta_f)^2}+\frac{|\mathbf{p}_i|^2c^2\sin^2\Theta_i}{(E_i-|\mathbf{p}_i|c\cos\Theta_i)^2}\right)\cdot A, && (15)\\
a_2 &:= \left(-\frac{2|\mathbf{p}_i||\mathbf{p}_f|c^2\sin\Theta_i\sin\Theta_f}{(E_i-|\mathbf{p}_i|c\cos\Theta_i)(E_f-|\mathbf{p}_f|c\cos\Theta_f)}\right)\cdot A, && (16)\\
a_3 &:= \left(\frac{4E_i^2|\mathbf{p}_f|^2\sin^2\Theta_f}{(E_f-|\mathbf{p}_f|c\cos\Theta_f)^2}+\frac{4E_f^2|\mathbf{p}_i|^2\sin^2\Theta_i}{(E_i-|\mathbf{p}_i|c\cos\Theta_i)^2}\right.\\
&+ \left.\frac{2\hbar^2\omega^2(|\mathbf{p}_i|^2\sin\Theta_i+|\mathbf{p}_f|^2\sin^2\Theta_f)}{(E_i-|\mathbf{p}_i|c\cos\Theta_i)(E_f-|\mathbf{p}_f|c\cos\Theta_f)}\right)\cdot A, && (17)\\
a_4 &:= \left(-\frac{|\mathbf{p}_i||\mathbf{p}_f|\sin\Theta_i\sin\Theta_f(4E_i^2+4E_f^2)}{(E_i-|\mathbf{p}_i|c\cos\Theta_i)(E_f-|\mathbf{p}_f|c\cos\Theta_f)}\right)\cdot A. && (18)
\end{aligned}$$

With (12) - (18), Eq. (1) can be written as:

$$\begin{aligned}
\frac{d^4\sigma}{d\omega\Omega_i d\Omega_f d\Phi} &= \frac{a_1}{\alpha\cos\Phi+\beta}+\frac{a_2\cos\Phi}{\alpha\cos\Phi+\beta}\\
&+ \frac{a_3}{(\alpha\cos\Phi+\beta)^2}+\frac{a_4\cos\Phi}{(\alpha\cos\Phi+\beta)^2}; && (19)
\end{aligned}$$

thus the integration over Φ simply reads

$$\begin{aligned}
\frac{d^3\sigma}{d\omega d\Omega_i d\Omega_f} &= \int_0^{2\pi} d\Phi\left[\frac{a_1}{\alpha\cos\Phi+\beta}+\frac{a_2\cos\Phi}{\alpha\cos\Phi+\beta}\right.\\
&+ \left.\frac{a_3}{(\alpha\cos\Phi+\beta)^2}+\frac{a_4\cos\Phi}{(\alpha\cos\Phi+\beta)^2}\right] && (20)
\end{aligned}$$

where $a_i,\ i \in \{1, \ldots, 4\}, \alpha$ and β still depend on Θ_f and Θ_i. These integrals can be calculated with the help of the residue theorem which is reviewed briefly in Appendix A. If $R(x, y) : \mathbb{R}^2 \to \mathbb{R}$ is a rational function without poles on the unit circle $x^2 + y^2 = 1$, then

$$\int\limits_0^{2\pi} R(\cos\Phi, \sin\Phi) d\Phi = 2\pi i \sum_{|z|<1} \mathrm{Res}(f, z) \tag{21}$$

where f is a complex function which is defined as

$$f(z) := \frac{1}{iz} R\left(\frac{1}{2}\left(z + \frac{1}{z}\right), \frac{1}{2i}\left(z - \frac{1}{z}\right)\right). \tag{22}$$

The residuum of a pole z_j of order n is defined as

$$\mathrm{Res}(f, z_j) = \frac{1}{(n-1)!} \lim_{z \to z_j} \frac{d^{n-1}}{dz^{n-1}} \Big[(z - z_j) f(z)\Big]. \tag{23}$$

To integrate the functions in Eq. (20), we write

$$\begin{aligned} R_1(x, y) &:= \frac{a_1}{\alpha x + \beta}, & (24)\\ R_2(x, y) &:= \frac{a_2 x}{\alpha x + \beta}, & (25)\\ R_3(x, y) &:= \frac{a_3}{(\alpha x + \beta)^2}, & (26)\\ R_4(x, y) &:= \frac{a_4 x}{(\alpha x + \beta)^2}; & (27) \end{aligned}$$

and get from (22)

$$\begin{aligned} f_1(z) &= \frac{2a_1}{i(\alpha z^2 + 2\beta z + \alpha)}, & (28)\\ f_2(z) &= \frac{a_2 z^2 + a_2}{zi(\alpha z^2 + 2\beta z + \alpha)}, & (29)\\ f_3(z) &= \frac{4a_3 z}{i\left(\alpha z^2 + 2\beta z + \alpha\right)^2}, & (30)\\ f_4(z) &= \frac{2a_4(z^2 + 1)}{i\left(\alpha z^2 + 2\beta z + \alpha\right)^2}. & (31) \end{aligned}$$

The poles of the functions $f_i(z)$ in (28) - (31) are given by

$$z_{1,2} = -\frac{\beta}{\alpha} \pm \sqrt{\left(\frac{\beta}{\alpha}\right)^2 - 1}. \tag{32}$$

For $f_{1,2}$ poles are of order one and for $f_{3,4}$ of order two. In addition f_2 has a pole at

$$z_3 = 0. \tag{33}$$

According to (21) one needs poles with $|z_i| < 1$. For z_3 it is quite clear that $|z_3| = 0 < 1$. As the angles Θ_i and Θ_f are between 0 and π, the expression $\alpha > 0$ in Eq. (12) and $\beta < 0$ in Eq. (13). Therefore β/α in Eq. (32) is a negative real number. Furthermore $\cos\Theta_f > -1$ and $\cos\Theta_i, \sin\Theta_i, \sin\Theta_f < 1$. Thus

$$\begin{aligned}
& -\beta - \alpha && (34)\\
= \;& \mathbf{p}_i^2 + \mathbf{p}_f^2 + \left(\frac{\hbar}{c}\omega\right)^2 + 2\frac{\hbar}{c}\omega|\mathbf{p}_f|\cos\Theta_f - 2\frac{\hbar}{c}\omega|\mathbf{p}_i|\cos\Theta_i \\
- \;& 2|\mathbf{p}_i||\mathbf{p}_f|\cos\Theta_i\cos\Theta_f - 2|\mathbf{p}_i||\mathbf{p}_f|\sin\Theta_i\sin\Theta_f && (35)\\
> \;& \mathbf{p}_i^2 + \mathbf{p}_f^2 + \left(\frac{\hbar}{c}\omega\right)^2 - 2\frac{\hbar}{c}\omega|\mathbf{p}_f| - 2\frac{\hbar}{c}\omega|\mathbf{p}_i| - 4|\mathbf{p}_i||\mathbf{p}_f| && (36)\\
> \;& \mathbf{p}_i^2 + \mathbf{p}_f^2 + \left(\frac{\hbar}{c}\omega\right)^2 > 0 && (37)\\
\Rightarrow \;& -\frac{\beta}{\alpha} > 1 && (38)
\end{aligned}$$

It follows immediately that $|z_1| > 1$ and $|z_2| < 1$. For all residua one obtains

$$\begin{aligned}
\mathrm{Res}(f_1, z_2) &= -\frac{a_1}{i}\frac{1}{\sqrt{\beta^2 - \alpha^2}}, && (39)\\
\mathrm{Res}(f_2, z_2) &= \frac{a_2\beta}{\alpha i}\frac{1}{\sqrt{\beta^2 - \alpha^2}}, && (40)\\
\mathrm{Res}(f_2, z_3) &= \frac{a_2}{\alpha i}, && (41)\\
\mathrm{Res}(f_3, z_2) &= -\frac{a_3\beta}{i}\frac{1}{(\sqrt{\beta^2 - \alpha^2})^3}, && (42)\\
\mathrm{Res}(f_4, z_2) &= a_4\alpha\frac{1}{(\sqrt{\beta^2 - \alpha^2})^3}. && (43)
\end{aligned}$$

With the knowledge of these residua and using (21), the integral in (20) can be calculated elementarily

$$\frac{d^3\sigma}{d\omega d\Omega_i d\Omega_f} = \frac{2\pi a_2}{\alpha} + \frac{2\pi}{\sqrt{\beta^2-\alpha^2}}\left[-a_1 + \frac{a_2\beta}{\alpha} - \frac{a_3\beta}{|\beta^2-\alpha^2|} + \frac{a_4\alpha}{|\beta^2-\alpha^2|}\right]. \qquad (44)$$

2.4. Integration over Θ_f

After having obtained an expression for the "triply" [1] differential cross section, there is still the integration over Θ_f left. This calculation is mainly straight forward, but rather tedious. Using expression (44), it is

$$\frac{d^2\sigma}{d\omega d\Omega_i} = \int_0^\pi d\Theta_f \left[\frac{2\pi a_2}{\alpha} + \frac{2\pi}{\sqrt{\beta^2-\alpha^2}}\left(-a_1 + \frac{a_2\beta}{\alpha} - \frac{a_3\beta}{|\beta^2-\alpha^2|} + \frac{a_4\alpha}{|\beta^2-\alpha^2|}\right)\right]\sin\Theta_f. \qquad (45)$$

Let's now consider the first integral of (45). If one inserts (12) and (16), it becomes

$$\int_0^\pi d\Theta_f \frac{2\pi a_2}{\alpha}\sin\Theta_f = -\frac{2\pi A c^2}{E_i - cp_i\cos\Theta_i}\int_0^\pi d\Theta_f \frac{\sin\Theta_f}{E_f - cp_f\cos\Theta_f} \qquad (46)$$

$$= -\frac{2\pi A c^2}{E_i - cp_i\cos\Theta_i}\int_{-1}^{+1} dx \frac{1}{E_f - cp_f x} \qquad (47)$$

where the substitution $x := \cos\Theta_f$ was made in the second step. (47) is rather simple and yields

$$\int_0^\pi d\Theta_f \frac{2\pi a_2}{\alpha}\sin\Theta_f = -\frac{2\pi A c}{(E_i - cp_i\cos\Theta_i)p_f}\ln\left(\frac{E_f + p_f c}{E_f - p_f c}\right). \qquad (48)$$

---

[1] Here "triply" really means the dependence on the photon frequency and two angles.

This was a quite simple calculation. All the other integrals can be calculated similarly, but with more effort. As another example let's consider the last integral. Before inserting (12), (13) and (18) one can define for simplicity

$$\begin{aligned} \Delta_1 &:= -\mathbf{p}_i^2 - \mathbf{p}_f^2 - \left(\frac{\hbar}{c}\omega\right)^2 + 2\frac{\hbar}{c}\omega|\mathbf{p}_i|\cos\Theta_i, && (49) \\ \Delta_2 &:= -2\frac{\hbar}{c}\omega|\mathbf{p}_f| + 2|\mathbf{p}_i||\mathbf{p}_f|\cos\Theta_i. && (50) \end{aligned}$$

The expression β from Eq. (13) is then

$$\beta = \Delta_1 + \Delta_2 \cos\Theta_f. \qquad (51)$$

Thus the regularly appearing term $\beta^2 - \alpha^2$ can be written as

$$\begin{aligned} \beta^2 - \alpha^2 &= (\Delta_2^2 + 4p_i^2 p_f^2 \sin^2\Theta_i)\cos^2\Theta_f + 2\Delta_1\Delta_2\cos\Theta_f \\ &+ (\Delta_1^2 - 4p_i^2 p_f^2 \sin^2\Theta_i) && (52) \\ &= \Box_1^2 \cos^2\Theta_f + 2\Delta_1\Delta_2\cos\Theta_f + \Box_2 && (53) \end{aligned}$$

where the definitions

$$\begin{aligned} \Box_1^2 &:= \Delta_2^2 + 4p_i^2 p_f^2 \sin^2\Theta_i, && (54) \\ \Box_2^2 &:= \Delta_1^2 - 4p_i^2 p_f^2 \sin^2\Theta_i && (55) \end{aligned}$$

have been introduced.

By using (12), (18) and (53), the last integral of (44) becomes

$$\begin{aligned} &\int_0^\pi d\Theta_f \frac{2\pi a_4 \alpha}{\sqrt{(\beta^2-\alpha^2)^3}} \sin\Theta_f = -\frac{16\pi A p_i^2 p_f^2 \sin^2\Theta_i (E_i^2 + E_f^2)}{E_i - cp_i\cos\Theta_i} \\ &\times \int_0^\pi d\Theta_f \frac{\sin^2\Theta_f}{\sqrt{(\Box_1^2\cos\Theta_f^2 + 2\Delta_1\Delta_2\cos\Theta_f + \Box_2^2)^3}(E_f - cp_f\cos\Theta_f)} \sin\Theta_f \\ & && (56) \\ &= -\frac{16\pi A p_i^2 p_f^2 \sin^2\Theta_i (E_i^2 + E_f^2)}{E_i - cp_i\cos\Theta_i} \\ &\times \int_{-1}^{+1} dx \frac{1-x^2}{\sqrt{(\Box_1^2 x^2 + 2\Delta_1\Delta_2 x + \Box_2^2)^3}(E_f - cp_f x)} && (57) \end{aligned}$$

where $x = \cos\Theta_f$ has been substituted again.

This integration can be performed elementarily by finding the indefinite integral

$$\begin{aligned}
& \frac{\Box_1^2 x^2 + 2\Delta_1\Delta_2 x + \Box_2^2}{\sqrt{(\Box_1^2 x^2 + 2\Delta_1\Delta_2 x + \Box_2^2)^3}(\Delta_1^2\Delta_2^2 - \Box_1^2\Box_2^2)(\Box_1^2 E_f^2 + 2\Delta_1\Delta_2 E_f p_f c + \Box_2^2 p_f c)} \times \\
\times \quad & \Big(-\Box_1^4 E_f x + \Box_2^4 p_f c + 2\Delta_1^2\Delta_2^2(E_f x - p_f c) + \Delta_1\Delta_2\Box_2^2(E_f + p_f cx) \\
- \quad & \Box_1^2(\Box_2^2(E_f x - p_f c)\Delta_1\Delta_2(E_f + p_f cx))\Big) \\
+ \quad & \frac{E_f^2 - p_f^2 c^2}{\sqrt{(\Box_1^2 E_f^2 + 2\Delta_1\Delta_2 E_f p_f c + \Box_2^2 p_f c)^3}} \ln\Big((E_f - p_f cx)(\Box_1^2 E_f x + \Box_2^2 p_f c \\
+ \quad & \Delta_1\Delta_2(E_f + p_f cx) + \sqrt{\Box_1^2 x^2 + 2\Delta_1\Delta_2 x + \Box_2^2} \times \\
\times \quad & \sqrt{\Box_1^2 E_f^2 + 2\Delta_1\Delta_2 E_f p_f c + \Box_2^2 p_f c})\Big),
\end{aligned} \tag{58}$$

by inserting $+1$ and -1 as upper and lower limit, using (54) and (55) and simplifying. The integral in (56) is then finally

$$\begin{aligned}
\int_0^\pi d\Theta_f \frac{2\pi a_4 \alpha}{\sqrt{(\beta^2 - \alpha^2)^3}} \sin\Theta_f \quad - \quad & \frac{16\pi A p_i^2 p_f^2 \sin^2\Theta_i (E_i^2 + E_f^2)}{E_i - cp_i \cos\Theta_i} \times \\
\times \quad & \Bigg[-\frac{2(\Delta_2 p_f c + \Delta_1 E_f)}{(-\Delta_2^2 + \Delta_1^2 - 4p_i^2 p_f^2 \sin^2\Theta_i)((\Delta_2 E_f + \Delta_1 p_f c)^2 + 4m^2c^4 p_i^2 p_f^2 \sin^2\Theta_i)} \\
+ \quad & \frac{m^2c^4}{\sqrt{((\Delta_2 E_f + \Delta_1 p_f c)^2 + 4m^2c^4 p_i^2 p_f^2 \sin^2\Theta_i)^3}} \times \\
\times \quad & \ln\Bigg(\Big((E_f - cp_f)(4p_i^2 p_f^2 \sin^2\Theta_i(-E_f - p_f c) + (\Delta_1 - \Delta_2)((\Delta_2 E_f + \Delta_1 p_f c) \\
- \quad & \sqrt{\Box_1^2 E_f^2 + 2\Delta_1\Delta_2 E_f p_f c + \Box_2^2 p_f c})\Big)\Big((E_f + cp_f)(4p_i^2 p_f^2 \sin^2\Theta_i(+E_f - p_f c) \\
+ \quad & (\Delta_1 + \Delta_2)((\Delta_2 E_f + \Delta_1 p_f c) - \sqrt{\Box_1^2 E_f^2 + 2\Delta_1\Delta_2 E_f p_f c + \Box_2^2 p_f c})\Big)^{-1}\Bigg)\Bigg].
\end{aligned} \tag{59}$$

All the other integrals can be calculated similarly where one always has to substitute $x = \cos\Theta_f$. With this technique the whole doubly differential cross section finally becomes

$$\frac{d^2\sigma(E_i, \omega, \Theta_i)}{d\omega d\Omega_i} = \sum_{j=1}^{6} I_j \tag{60}$$

with the following contributions:

$$
\begin{aligned}
I_1 &= \frac{2\pi A}{\sqrt{\Delta_2^2 + 4p_i^2 p_f^2 \sin^2\Theta_i}} \ln\left(\frac{\Delta_2^2 + 4p_i^2 p_f^2 \sin^2\Theta_i - \sqrt{\Delta_2^2 + 4p_i^2 p_f^2 \sin^2\Theta_i}(\Delta_1 + \Delta_2) + \Delta_1\Delta_2}{-\Delta_2^2 - 4p_i^2 p_f^2 \sin^2\Theta_i - \sqrt{\Delta_2^2 + 4p_i^2 p_f^2 \sin^2\Theta_i}(\Delta_1 - \Delta_2) + \Delta_1\Delta_2}\right) \\
&\times \left[1 + \frac{c\Delta_2}{p_f(E_i - cp_i\cos\Theta_i)} - \frac{p_i^2 c^2 \sin^2\Theta_i}{(E_i - cp_i\cos\Theta_i)^2} - \frac{2\hbar^2\omega^2 p_f\Delta_2}{c(E_i - cp_i\cos\Theta_i)(\Delta_2^2 + 4p_i^2 p_f^2 \sin^2\Theta_i)}\right], \qquad (61) \\
I_2 &= -\frac{2\pi A c}{p_f(E_i - cp_i\cos\Theta_i)} \ln\left(\frac{E_f + p_f c}{E_f - p_f c}\right), \qquad (62) \\
I_3 &= \frac{2\pi A}{\sqrt{(\Delta_2 E_f + \Delta_1 p_f c)^2 + 4m^2c^4 p_i^2 p_f^2 \sin^2\Theta_i}} \\
&\times \ln\Bigg(\Big((E_f + p_f c)(4p_i^2 p_f^2 \sin^2\Theta_i(E_f - p_f c) + (\Delta_1 + \Delta_2)((\Delta_2 E_f + \Delta_1 p_f c) \\
&- \sqrt{(\Delta_2 E_f + \Delta_1 p_f c)^2 + 4m^2c^4 p_i^2 p_f^2 \sin^2\Theta_i)))\Big)\Big((E_f - p_f c)(4p_i^2 p_f^2 \sin^2\Theta_i(-E_f - p_f c) \\
&+ (\Delta_1 - \Delta_2)((\Delta_2 E_f + \Delta_1 p_f c) - \sqrt{(\Delta_2 E_f + \Delta_1 p_f c)^2 + 4m^2c^4 p_i^2 p_f^2 \sin^2\Theta_i)))\Big)^{-1}\Bigg) \\
&\times \Bigg[-\frac{(\Delta_2^2 + 4p_i^2 p_f^2 \sin^2\Theta_i)(E_f^3 + E_f p_f^2 c^2) + p_f c(2(\Delta_1^2 - 4p_i^2 p_f^2 \sin^2\Theta_i)E_f p_f c + \Delta_1\Delta_2(3E_f^2 + p_f^2 c^2))}{(\Delta_2 E_f + \Delta_1 p_f c)^2 + 4m^2c^4 p_i^2 p_f^2 \sin^2\Theta_i} \\
&- \frac{c(\Delta_2 E_f + \Delta_1 p_f c)}{p_f(E_i - cp_i\cos\Theta_i)} \\
&- \frac{4E_i^2 p_f^2(2(\Delta_2 E_f + \Delta_1 p_f c)^2 - 4m^2c^4 p_i^2 p_f^2 \sin^2\Theta_i)(\Delta_1 E_f + \Delta_2 p_f c)}{((\Delta_2 E_f + \Delta_1 p_f c)^2 + 4m^2c^4 p_i^2 p_f^2 \sin^2\Theta_i)^2} \\
&+ \frac{8p_i^2 p_f^2 m^2 c^4 \sin^2\Theta_i(E_i^2 + E_f^2) - 2\hbar^2\omega^2 p_i^2 \sin^2\Theta_i p_f c(\Delta_2 E_f + \Delta_1 p_f c) + 2\hbar^2\omega^2 p_f m^2 c^3(\Delta_2 E_f + \Delta_1 p_f c)}{(E_i - cp_i\cos\Theta_i)((\Delta_2 E_f + \Delta_1 p_f c)^2 + 4m^2c^4 p_i^2 p_f^2 \sin^2\Theta_i)}\Bigg], \\
&\qquad (63) \\
I_4 &= -\frac{4\pi A p_f c(\Delta_2 E_f + \Delta_1 p_f c)}{(\Delta_2 E_f + \Delta_1 p_f c)^2 + 4m^2c^4 p_i^2 p_f^2 \sin^2\Theta_i} - \frac{16\pi E_i^2 p_f^2 A(\Delta_2 E_f + \Delta_1 p_f c)^2}{((\Delta_2 E_f + \Delta_1 p_f c)^2 + 4m^2c^4 p_i^2 p_f^2 \sin^2\Theta_i)^2}, \qquad (64) \\
I_5 &= \frac{4\pi A}{(-\Delta_2^2 + \Delta_1^2 - 4p_i^2 p_f^2 \sin^2\Theta_i)((\Delta_2 E_f + \Delta_1 p_f c)^2 + 4m^2c^4 p_i^2 p_f^2 \sin^2\Theta_i)} \\
&\times \Bigg[\frac{\hbar^2\omega^2 p_f^2}{E_i - cp_i\cos\Theta_i} \\
&\times \frac{E_f[2\Delta_2^2(\Delta_2^2 - \Delta_1^2) + 8p_i^2 p_f^2 \sin^2\Theta_i(\Delta_2^2 + \Delta_1^2)] + p_f c[2\Delta_1\Delta_2(\Delta_2^2 - \Delta_1^2) - 16\Delta_1\Delta_2 p_i^2 p_f^2 \sin^2\Theta_i]}{\Delta_2^2 + 4p_i^2 p_f^2 \sin^2\Theta_i} \\
&+ \frac{2\hbar^2\omega^2 \sin^2\Theta_i(2\Delta_1\Delta_2 p_f c + 2\Delta_2^2 E_f + 8p_i^2 p_f^2 \sin^2\Theta_i E_f)}{E_i - cp_i\cos\Theta_i} \\
&+ \frac{2E_i^2 p_f^2\{2(\Delta_2^2 - \Delta_1^2)(\Delta_2 E_f + \Delta_1 p_f c)^2 + 8p_i^2 p_f^2 \sin^2\Theta_i[(\Delta_1^2 + \Delta_2^2)(E_f^2 + p_f^2 c^2) + 4\Delta_1\Delta_2 E_f p_f c]\}}{((\Delta_2 E_f + \Delta_1 p_f c)^2 + 4m^2c^4 p_i^2 p_f^2 \sin^2\Theta_i)} \\
&+ \frac{8p_i^2 p_f^2 \sin^2\Theta_i(E_i^2 + E_f^2)(\Delta_2 p_f c + \Delta_1 E_f)}{E_i - cp_i\cos\Theta_i}\Bigg], \qquad (65) \\
I_6 &= \frac{16\pi E_f^2 p_i^2 \sin^2\Theta_i A}{(E_i - cp_i\cos\Theta_i)^2(-\Delta_2^2 + \Delta_1^2 - 4p_i^2 p_f^2 \sin^2\Theta_i)}. \qquad (66)
\end{aligned}
$$

Eq. (60) depends explicitly on E_i, ω and Θ_i while E_f and p_f are functions of E_i and ω through (2) and (3). (60) is the final result of the integration of (1) over Φ and Θ_f with the help of the residue theorem and some basic calculations. Now this result can be used both as input for Monte Carlo code and for discussing some basic properties of the behaviour of produced

Bremsstrahlung photons.

Actually (60) is also valid for $\Theta_i = 0$, as will be shown in the next section, but the simple way just to set $\Theta_i = 0$ in (60) will fail, especially for numerical purposes, because the logarithmic part in (61) tends to $\ln(0/0)$ for $\Theta_i \to 0$ and so fails for numerical applications. Thus we need an additional expression for $\Theta_i = 0$ which has to be consistent with (60).

2.5. Special limits: $\Theta_i = 0, \pi$ *and* $\hbar\omega \to E_{kin,i}$

For some special cases the integration of (1) over Φ and Θ_f is easier. This information can also be used to verify (60) by checking consistency and use them for Monte Carlo codes.

2.5.1. $\Theta_i = 0$ *or* $\Theta_i = \pi$

If one is only interested in forward and backward scattering, one can set $\Theta_i = 0$ or $\Theta_i = \pi$ before integrating; then (1) becomes

$$\begin{aligned}\frac{d^4\sigma}{d\omega d\Omega_i d\Omega_f d\Phi} &= \frac{Z^2\alpha_{fine}^3 h^2}{(2\pi)^2}\frac{|\mathbf{p}_f|}{|\mathbf{p}_i|}\frac{1}{\omega}\frac{1}{|\mathbf{q}|^4} \\ &\times \left(\frac{\mathbf{p}_f^2\sin^2\Theta_f}{(E_f - c|\mathbf{p}_f|\cos\Theta_f)^2}\left(4E_i^2 - c^2\mathbf{q}^2\right)\right. \\ &+ \left. 2\,\hbar^2\omega^2\frac{\mathbf{p}_f^2\sin^2\Theta_f}{(E_f - c|\mathbf{p}_f|\cos\Theta_f)(E_i \mp c|\mathbf{p}_i|\cos\Theta_i)}\right) \end{aligned} \tag{67}$$

where the momentum $\mathbf{q}$ of the virtual photon can be written as

$$-\mathbf{q}^2 = -\mathbf{p}_i^2 - \mathbf{p}_f^2 - \left(\frac{\hbar}{c}\omega\right)^2 - 2\frac{\hbar}{c}|\mathbf{p}_f|\cos\Theta_f \pm 2\frac{\hbar}{c}\omega|\mathbf{p}_i| \pm 2|\mathbf{p}_i||\mathbf{p}_f|\cos\Theta_f. \tag{68}$$

Here the upper sign corresponds to $\Theta_i = 0$ and the lower one to $\Theta_i = \pi$.

As (67) and (68) do not depend on Φ at all, the Φ integration simply gives a factor of 2π, and (67) becomes

$$
\begin{aligned}
\frac{d^3\sigma}{d\omega d\Omega_i d\Omega_f} &= \frac{Z^2\alpha_{fine}^3 h^2}{2\pi}\frac{|\mathbf{p}_f|}{|\mathbf{p}_i|}\frac{1}{\omega}\frac{1}{|\mathbf{q}|^4} \\
&\times \left(\frac{\mathbf{p}_f^2\sin^2\Theta_f}{(E_f - c|\mathbf{p}_f|\cos\Theta_f)^2}\left(4E_i^2 - c^2\mathbf{q}^2\right)\right. \\
&+ \left. 2\,\hbar^2\omega^2\frac{\mathbf{p}_f^2\sin^2\Theta_f}{(E_f - c|\mathbf{p}_f|\cos\Theta_f)(E_i \mp c|\mathbf{p}_i|\cos\Theta_i)}\right). \qquad (69)
\end{aligned}
$$

Finally this expression has to be integrated over Θ_f in order to obtain the doubly differential cross section. Similarly to the total integration of (45) it is convenient to define

$$
\begin{aligned}
\tilde{\Delta}_1 &:= -\left(p_i \mp \frac{\hbar}{c}\omega\right)^2 - p_f^2, \qquad (70) \\
\tilde{\Delta}_2 &:= -2\frac{\hbar}{c}\omega p_f \pm 2p_i p_f \qquad (71)
\end{aligned}
$$

where $\tilde{\Delta}_{1,2} = \Delta_{1,2}(\Theta_i = 0, \pi), j \in \{1,2\}$, with definitions (49) and (50). Eq. (68) can then be rewritten as

$$
-\mathbf{q}^2 = \tilde{\Delta}_1 + \tilde{\Delta}_2\cos\Theta_f \qquad (72)
$$

and

$$
\begin{aligned}
\frac{d^2\sigma}{d\omega d\Omega_i} &= \frac{Z^2\alpha_{fine}^3 h^2}{2\pi}\frac{|\mathbf{p}_f|}{|\mathbf{p}_i|}\frac{1}{\omega}\int_0^\pi d\Theta_f\left[\frac{|\mathbf{p}_f|^2c^2\sin^2\Theta_f}{(E_f - |\mathbf{p}_f|c\cos\Theta_f)^2(\tilde{\Delta}_1 + \tilde{\Delta}_2\cos\Theta_f)}\right. \\
&+ \frac{4E_i^2|\mathbf{p}_f|^2\sin^2\Theta_f}{(E_f - |\mathbf{p}_f|c\cos\Theta_f)^2(\tilde{\Delta}_1 + \tilde{\Delta}_2\cos\Theta_f)^2} \\
&+ \left.\frac{2\hbar^2\omega^2|\mathbf{p}_f|^2\sin^2\Theta_f}{(E_i \mp c|\mathbf{p}_i|)(E_f - |\mathbf{p}_f|c\cos\Theta_f)(\tilde{\Delta}_1 + \tilde{\Delta}_2\cos\Theta_f)^2}\right]\sin\Theta_f
\end{aligned}
$$

(73)

where the integration is rather elementary and can be performed by substituting $x = \cos\Theta_f$ again. Thus (73) yields

$$
\begin{aligned}
& \frac{d^2\sigma}{d\omega d\Omega_i}(E_i, \omega, \Theta_i = 0, \pi) = \frac{Z^2\alpha^3 h^2}{2\pi}\frac{|\mathbf{p}_f|}{|\mathbf{p}_i|}\frac{1}{\omega}\left[-\frac{2|\mathbf{p}_f|c}{\tilde{\Delta}_2 E_f + \tilde{\Delta}_1|\mathbf{p}_f|c}\right. \\
+ \quad & \frac{|\mathbf{p}_f|^2c^2(-\tilde{\Delta}_1^2 + \tilde{\Delta}_2^2)}{\tilde{\Delta}_2(\tilde{\Delta}_2 E_f + \tilde{\Delta}_1|\mathbf{p}_f|c)^2}\ln\left(\frac{\tilde{\Delta}_1 + \tilde{\Delta}_2}{\tilde{\Delta}_1 - \tilde{\Delta}_2}\right) \\
+ \quad & \frac{2\tilde{\Delta}_1 E_f|\mathbf{p}_f|c + \tilde{\Delta}_2(E_f^2 + |\mathbf{p}_f|^2c^2)}{(\tilde{\Delta}_2 E_f + \tilde{\Delta}_1|\mathbf{p}_f|c)^2}\ln\left(\frac{E_f + |\mathbf{p}_f|c}{E_f - |\mathbf{p}_f|c}\right) \\
- \quad & \frac{16E_i^2|\mathbf{p}_f|^2}{(\tilde{\Delta}_2 E_f + \tilde{\Delta}_1|\mathbf{p}_f|c)^2} - \frac{4\hbar^2|\mathbf{p}_f|^2\omega^2}{(\tilde{\Delta}_2 E_f + \tilde{\Delta}_1|\mathbf{p}_f|c)(E_i \mp c|\mathbf{p}_i|)\tilde{\Delta}_2} \\
- \quad & \frac{8E_i^2|\mathbf{p}_f|^2(\tilde{\Delta}_1 E_f + \tilde{\Delta}_2|\mathbf{p}_f|c)}{(\tilde{\Delta}_2 E_f + \tilde{\Delta}_1|\mathbf{p}_f|c)^3}\ln\left(\frac{(\tilde{\Delta}_1 - \tilde{\Delta}_2)(E_f - |\mathbf{p}_f|c)}{(\tilde{\Delta}_1 + \tilde{\Delta}_2)(E_f + |\mathbf{p}_f|c)}\right) \\
+ \quad & \frac{2\hbar^2|\mathbf{p}_f|^2\omega^2(2\tilde{\Delta}_1\tilde{\Delta}_2 E_f + \tilde{\Delta}_1^2|\mathbf{p}_f|c + \tilde{\Delta}_2^2|\mathbf{p}_f|c)}{(\tilde{\Delta}_2 E_f + \tilde{\Delta}_1|\mathbf{p}_f|c)^2(E_i \mp c|\mathbf{p}_i|)\tilde{\Delta}_2^2}\ln\left(\frac{\tilde{\Delta}_1 + \tilde{\Delta}_2}{\tilde{\Delta}_1 - \tilde{\Delta}_2}\right) \\
+ \quad & \left.\frac{2\hbar^2|\mathbf{p}_f|\omega^2(E_f^2 - c^2|\mathbf{p}_f|^2)}{(\tilde{\Delta}_2 E_f + \tilde{\Delta}_1|\mathbf{p}_f|c)^2(E_i \mp c|\mathbf{p}_i|)c}\ln\left(\frac{E_f - |\mathbf{p}_f|c}{E_f + |\mathbf{p}_f|c}\right)\right]. \qquad (74)
\end{aligned}
$$

This expression is much simpler than (60), but only valid for $\Theta_i = 0$ or $\Theta_i = \pi$. Actually this expression can also be obtained by calculating the limit $\Theta_i \to 0$ or $\Theta_i \to \pi$ in (60); hence both expressions are consistent. The reader interested in details of this calculation, is referred to Appendix B.

2.5.2. $\hbar\omega \to E_{kin,i}$

The other case which can be investigated easily is when almost all kinetic energy of the incident electron is transferred to the emitted photon, i.e.,

$$
E_f = E_i - \hbar\omega = E_{kin,i} + m_e c^2 - \hbar\omega \xrightarrow{\hbar\omega\to E_{kin,i}} m_e c^2 \qquad (75)
$$

and

$$
|\mathbf{p}_f| = \sqrt{\frac{E_f^2}{c^2} - m_e^2c^2} \xrightarrow{\hbar\omega\to E_{kin,i}} \sqrt{\frac{m_e^2c^4}{c^2} - m_e^2c^2} \equiv 0 \qquad (76)
$$

and consequently from Eq. (9)

$$-\mathbf{q}^2 \xrightarrow{\hbar\omega\to E_{kin,i}} -\mathbf{p}_i^2 - \left(\frac{\hbar}{c}\omega\right)^2 + 2\frac{\hbar}{c}\omega|\mathbf{p}_i|\cos\Theta_i \qquad =: \qquad \delta \tag{77}$$

$$\Rightarrow \mathbf{q}^4 \quad \xrightarrow{\hbar\omega\to E_{kin,i}} \quad \delta^2. \tag{78}$$

With these limits it follows for the triply differential cross section (1)

$$\begin{aligned} \frac{d^4\sigma}{d\omega d\Omega_i d\Omega_f d\Phi} \quad \xrightarrow{\hbar\omega\to E_{kin,i}} \quad & \frac{Z^2\alpha_{fine}^3 h^2}{(2\pi)^2}\frac{|\mathbf{p}_f|}{|\mathbf{p}_i|}\frac{1}{\omega}\frac{1}{\delta^2}\left[\frac{|\mathbf{p}_i|^2\sin^2\Theta_i}{(E_i - c|\mathbf{p}_i|\cos\Theta_i)^2}\right. \\ \times \qquad & \left.(4E_f^2 + \delta c^2) + 2\,\hbar^2\omega^2\frac{|\mathbf{p}_i|^2\sin^2\Theta_i}{(E_i - c|\mathbf{p}_i|\cos\Theta_i)E_f}\right]. \end{aligned} \tag{79}$$

Actually (79) depends neither on Φ, nor on Θ_f. Therefore

$$\int_0^{2\pi} d\Phi \int_0^{\pi} \sin\Theta_i d\Theta_i = 4\pi \tag{80}$$

which leads to a very simple expression for the doubly differential cross section

$$\begin{aligned} \frac{d^2\sigma}{d\omega d\Omega_i} \xrightarrow{\hbar\omega\to E_{kin,i}} \qquad & \frac{Z^2\alpha^3 h^2}{\pi}\frac{|\mathbf{p}_f|}{|\mathbf{p}_i|}\frac{1}{\omega}\frac{1}{\delta^2}\left[\frac{|\mathbf{p}_i|^2\sin^2\Theta_i}{(E_i - c|\mathbf{p}_i|\cos\Theta_i)^2}(4E_f^2 + \delta c^2)\right. \\ + \quad & \left. 2\,\hbar^2\omega^2\frac{|\mathbf{p}_i|^2\sin^2\Theta_i}{(E_i - c|\mathbf{p}_i|\cos\Theta_i)E_f}\right]. \end{aligned} \tag{81}$$

It seems that taking the limit $\hbar\omega \to E_{kin,i}$ contradicts Eq. (11) as the energy of the emitted electron should be larger than 1 keV (11), too. But (81) can be used for two purposes.

As (81) can be obtained, as well, by taking the limit $|\mathbf{p}_f| \to 0$ in (60), the complicated expression (60) is verified. For further details the reader is referred to Appendix C. Although this formula is strictly valid only for $\hbar\omega/E_{kin,i} \to 1$ we will, however, see in section 4.1.4 that this cross section can also be used for calculating the most probable scattering angle for almost every photon energy.

3. Pair production

Pairs of electrons and positrons can be produced if a photon interacts with the nucleus of an atom. This process is related by some symmetry to the production of Bremsstrahlung photons. Bremsstrahlung occurs when an electron is affected by the nucleus of an atom, scattered and then emits a photon. So there are three real particles involved: incident electron, scattered electron and emitted photon. As the photon has no antiparticle one can change the time direction of the photon. For antimatter it is well known that antiparticles can be interpreted as the corresponding particles moving back in time. So one can substitute the incident electron by an positron moving forward in time. Thus by substituting emitted photon by incident photon and incident electron by emitted positron (due to time reversal and changing its charge) it is possible to describe pair production from Bremsstrahlung. Thus the emitted photon in the Bremsstrahlung process has to be substituted by the incident photon from the nucleus and the incident electron by the produced positron. With these two replacements one gets the differential cross section for pair production (Heitler, 1944; Greiner and Reinhardt, 1995)

$$
\begin{aligned}
d^4\sigma &= \frac{Z^2\alpha_{fine}^3 c^2}{(2\pi)^2 h}|\mathbf{p}_+||\mathbf{p}_-|\frac{dE_+}{\omega^3}\frac{d\Omega_+ d\Omega_- d\Phi}{|\mathbf{q}|^4}\times \\
&\times \left[-\frac{\mathbf{p}_-^2\sin^2\Theta_-}{(E_- - c|\mathbf{p}_-|\cos\Theta_-)^2}\left(4E_+^2 - c^2\mathbf{q}^2\right)\right. \\
&- \frac{\mathbf{p}_+^2\sin^2\Theta_+}{(E_+ - c|\mathbf{p}_+|\cos\Theta_+)^2}\left(4E_-^2 - c^2\mathbf{q}^2\right) \\
&+ 2\hbar^2\omega^2\frac{\mathbf{p}_+^2\sin^2\Theta_+ + \mathbf{p}_-^2\sin^2\Theta_-}{(E_+ - c|\mathbf{p}_+|\cos\Theta_+)(E_- - c|\mathbf{p}_-|\cos\Theta_-)} \\
&+ \left. 2\,\frac{|\mathbf{p}_+||\mathbf{p}_-|\sin\Theta_+\sin\Theta_-\cos\Phi}{(E_+ - c|\mathbf{p}_+|\cos\Theta_+)(E_- - c|\mathbf{p}_-|\cos\Theta_-)}\left(2E_+^2 + 2E_-^2 - c^2\mathbf{q}^2\right)\right],
\end{aligned}
\tag{82}
$$

where Z, α_{fine}, h, $\hbar$ and c are the same parameters as in Eq. (1). ω is the frequency of the incident photon, $E_\pm$ and $p_\pm$ are the total energy and the momentum of the positron/electron with

$$E_\pm = \sqrt{\mathbf{p}_\pm^2 c^2 + m_e^2 c^4}. \tag{83}$$

Similarly to (1) there are three angles, $\Theta_\pm$ between the direction of the photon and the positron/electron direction, $\Theta_+ = \sphericalangle(\mathbf{p}_+, \mathbf{k}), \Theta_- = \sphericalangle(\mathbf{p}_-, \mathbf{k})$, and Φ

is the angle between the scattering planes $(\mathbf{p}_+, \mathbf{k})$ and $(\mathbf{p}_-, \mathbf{k})$. The absolute value of the momentum of the virtual photon is

$$\begin{aligned} -\mathbf{q}^2 &= -|\mathbf{p}_+|^2 - |\mathbf{p}_-|^2 - \left(\frac{\hbar}{c}\omega\right)^2 + 2|\mathbf{p}_+|\frac{\hbar}{c}\omega\cos\Theta_+ + 2|\mathbf{p}_-|\frac{\hbar}{c}\omega\cos\Theta_- \\ &- 2|\mathbf{p}_+||\mathbf{p}_-|(\cos\Theta_+\cos\Theta_- + \sin\Theta_+\sin\Theta_-\cos\Phi). \end{aligned} \tag{84}$$

Algebraically one obtains (82) from (1) by replacing

$$E_f \rightarrow E_-, \tag{85}$$
$$E_i \rightarrow -E_+, \tag{86}$$
$$\mathbf{p}_i \rightarrow -\mathbf{p}_+, \tag{87}$$
$$\mathbf{p}_f \rightarrow \mathbf{p}_-, \tag{88}$$
$$\omega \rightarrow -\omega, \tag{89}$$
$$\Theta_i \rightarrow \pi - \Theta_+, \tag{90}$$
$$\Theta_f \rightarrow \Theta_-, \tag{91}$$
$$\Phi \rightarrow \Phi - \pi \tag{92}$$

where the quantities on the left hand side are for Bremsstrahlung, and those on the right hand side for pair production. At the end one has to multiply with an additional factor to get the correct prefactor. With all the mentioned substitutions it is

$$d^4\sigma_{brems} \leftarrow \frac{h^3\omega^2}{|\mathbf{p}_+|^2c^2}\frac{d\omega}{dE_+}d^4\sigma_{pair}, \tag{93}$$

Because of this symmetry the results for pair production follow easily from those for Bremsstrahlung.

The direction of the positron relative to the incident photon is given by integrating (82) over Φ and Θ_-. But this is the same exercise as to integrate (1) over Φ and Θ_f. Because of the symmetry between Bremsstrahlung and pair production one can take (60) and substitute (85) - (92) to obtain a doubly differential cross section

$$\frac{d^2\sigma(E_+, \omega, \Theta_+)}{dE_+ d\Omega_+} = \sum_{j=1}^{6} I_j \tag{94}$$

with the following contributions

$$\begin{aligned}
I_1 &= \frac{2\pi A}{\sqrt{(\Delta_2^{(p)})^2 + 4p_+^2 p_-^2 \sin^2\Theta_i}} \\
&\times \ln\left(\frac{(\Delta_2^{(p)})^2 + 4p_+^2 p_-^2 \sin^2\Theta_i - \sqrt{(\Delta_2^{(p)})^2 + 4p_+^2 p_-^2 \sin^2\Theta_i}(\Delta_1^{(p)} + \Delta_2^{(p)}) + \Delta_1^{(p)}\Delta_2^{(p)}}{-(\Delta_2^{(p)})^2 - 4p_+^2 p_-^2 \sin^2\Theta_i - \sqrt{(\Delta_2^{(p)})^2 + 4p_+^2 p_-^2 \sin^2\Theta_i}(\Delta_1^{(p)} - \Delta_2^{(p)}) + \Delta_1^{(p)}\Delta_2^{(p)}}\right) \\
&\times \left[-1 - \frac{c\Delta_2^{(p)}}{p_-(E_+ - cp_+\cos\Theta_i)} + \frac{p_+^2 c^2 \sin^2\Theta_i}{(E_+ - cp_+\cos\Theta_i)^2} - \frac{2\hbar^2\omega^2 p_-\Delta_2^{(p)}}{c(E_+ - cp_+\cos\Theta_i)((\Delta_2^{(p)})^2 + 4p_+^2 p_-^2 \sin^2\Theta_i)}\right],
\end{aligned} \tag{95}$$

$$I_2 = \frac{2\pi A c}{p_-(E_+ - cp_+\cos\Theta_i)} \ln\left(\frac{E_- + p_- c}{E_- - p_- c}\right), \tag{96}$$

$$\begin{aligned}
I_3 &= \frac{2\pi A}{\sqrt{(\Delta_2^{(p)} E_- + \Delta_1^{(p)} p_- c)^2 + 4m^2c^4 p_+^2 p_-^2 \sin^2\Theta_i}} \\
&\times \ln\Bigg(\bigg((E_- + p_- c)(4p_+^2 p_-^2 \sin^2\Theta_i(E_- - p_- c) + (\Delta_1^{(p)} + \Delta_2^{(p)})((\Delta_2^{(p)} E_- + \Delta_1^{(p)} p_- c) \\
&- \sqrt{(\Delta_2^{(p)} E_- + \Delta_1^{(p)} p_- c)^2 + 4m^2c^4 p_+^2 p_-^2 \sin^2\Theta_i}))\bigg)\bigg((E_- - p_- c)(4p_+^2 p_-^2 \sin^2\Theta_i(-E_- - p_- c) \\
&+ (\Delta_1^{(p)} - \Delta_2^{(p)})((\Delta_2^{(p)} E_- + \Delta_1^{(p)} p_- c) - \sqrt{(\Delta_2^{(p)} E_- + \Delta_1^{(p)} p_- c)^2 + 4m^2c^4 p_+^2 p_-^2 \sin^2\Theta_i}))\bigg)^{-1}\Bigg) \\
&\times \Bigg[\frac{c(\Delta_2^{(p)} E_- + \Delta_1^{(p)} p_- c)}{p_-(E_+ - cp_+\cos\Theta_i)} \\
&+ \Big[((\Delta_2^{(p)})^2 + 4p_+^2 p_-^2 \sin^2\Theta_i)(E_-^3 + E_- p_- c) + p_- c(2((\Delta_1^{(p)})^2 - 4p_+^2 p_-^2 \sin^2\Theta_i)E_- p_- c \\
&+ \Delta_1^{(p)}\Delta_2^{(p)}(3E_-^2 + p_-^2 c^2))\Big]\Big[(\Delta_2^{(p)} E_- + \Delta_1^{(p)} p_- c)^2 + 4m^2c^4 p_+^2 p_-^2 \sin^2\Theta_i\Big]^{-1} \\
&+ \Big[-8p_+^2 p_-^2 m^2 c^4 \sin^2\Theta_i(E_+^2 + E_-^2) - 2\hbar^2\omega^2 p_+^2 \sin^2\Theta_i p_- c(\Delta_2^{(p)} E_- + \Delta_1^{(p)} p_- c) \\
&+ 2\hbar^2\omega^2 p_- m^2 c^3(\Delta_2^{(p)} E_- + \Delta_1^{(p)} p_- c)\Big]\Big[(E_+ - cp_+\cos\Theta_i)((\Delta_2^{(p)} E_- + \Delta_1^{(p)} p_- c)^2 + 4m^2c^4 p_+^2 p_-^2 \sin^2\Theta_i)\Big]^{-1} \\
&+ \frac{4E_+^2 p_-^2(2(\Delta_2^{(p)} E_- + \Delta_1^{(p)} p_- c)^2 - 4m^2c^4 p_+^2 p_-^2 \sin^2\Theta_i)(\Delta_1^{(p)} E_- + \Delta_2^{(p)} p_- c)}{((\Delta_2^{(p)} E_- + \Delta_1^{(p)} p_- c)^2 + 4m^2c^4 p_+^2 p_-^2 \sin^2\Theta_i)^2}\Bigg],
\end{aligned} \tag{97}$$

$$I_4 = \frac{4\pi A p_- c(\Delta_2^{(p)} E_- + \Delta_1^{(p)} p_- c)}{(\Delta_2^{(p)} E_- + \Delta_1^{(p)} p_- c)^2 + 4m^2c^4 p_+^2 p_-^2 \sin^2\Theta_i} + \frac{16\pi E_+^2 p_-^2 A(\Delta_2^{(p)} E_- + \Delta_1^{(p)} p_- c)^2}{((\Delta_2^{(p)} E_- + \Delta_1^{(p)} p_- c)^2 + 4m^2c^4 p_+^2 p_-^2 \sin^2\Theta_i)^2}, \tag{98}$$

$$\begin{aligned}
I_5 &= \frac{4\pi A}{(-(\Delta_2^{(p)})^2 + (\Delta_1^{(p)})^2 - 4p_+^2 p_-^2 \sin^2\Theta_i)((\Delta_2^{(p)} E_- + \Delta_1^{(p)} p_- c)^2 + 4m^2c^4 p_+^2 p_-^2 \sin^2\Theta_i)} \\
&\times \Bigg[\frac{\hbar^2\omega^2 p_-^2}{E_+ cp_+ \cos\Theta_i}\Big[E_-[2(\Delta_2^{(p)})^2((\Delta_2^{(p)})^2 - (\Delta_1^{(p)})^2) + 8p_+^2 p_-^2 \sin^2\Theta_i((\Delta_2^{(p)})^2 + (\Delta_1^{(p)})^2)] \\
&+ p_- c[2\Delta_1^{(p)}\Delta_2^{(p)}((\Delta_2^{(p)})^2 - (\Delta_1^{(p)})^2) - 16\Delta_1^{(p)}\Delta_2^{(p)} p_+^2 p_-^2 \sin^2\Theta_i]\Big]\Big[(\Delta_2^{(p)})^2 + 4p_+^2 p_-^2 \sin^2\Theta_i\Big]^{-1} \\
&+ \frac{2\hbar^2\omega^2 \sin^2\Theta_i(2\Delta_1^{(p)}\Delta_2^{(p)} p_- c + 2(\Delta_2^{(p)})^2 E_- + 8p_+^2 p_-^2 \sin^2\Theta_i E_-)}{E_+ - cp_+\cos\Theta_i} \\
&- \Big[2E_+^2 p_-^2\{2((\Delta_2^{(p)})^2 - (\Delta_1^{(p)})^2)(\Delta_2^{(p)} E_- + \Delta_1^{(p)} p_- c)^2 + 8p_+^2 p_-^2 \sin^2\Theta_i[((\Delta_1^{(p)})^2 + (\Delta_2^{(p)})^2)(E_-^2 + p_-^2 c^2) \\
&+ 4\Delta_1^{(p)}\Delta_2^{(p)} E_- p_- c]\}\Big]\Big[(\Delta_2^{(p)} E_- + \Delta_1^{(p)} p_- c)^2 + 4m^2c^4 p_+^2 p_-^2 \sin^2\Theta_i\Big]^{-1} \\
&- \frac{8p_+^2 p_-^2 \sin^2\Theta_i(E_+^2 + E_-^2)(\Delta_2^{(p)} p_- c + \Delta_1^{(p)} E_-)}{E_+ - cp_+\cos\Theta_i}\Bigg],
\end{aligned} \tag{99}$$

$$I_6 = -\frac{16\pi E_-^2 p_+^2 \sin^2\Theta_i A}{(E_+ - cp_+\cos\Theta_i)^2(-(\Delta_2^{(p)})^2 + (\Delta_1^{(p)})^2 - 4p_+^2 p_-^2 \sin^2\Theta_+)} \tag{100}$$

with

$$A = \frac{Z^2 \alpha_{fine}^3 c^2}{(2\pi)^2 h} \frac{|\mathbf{p}_+||\mathbf{p}_-|}{\omega^3}, \tag{101}$$

and with $\Delta_1^{(p)}, \Delta_2^{(p)}$ defined as

$$\Delta_1^{(p)} \quad := \quad -|\mathbf{p}_+|^2 - |\mathbf{p}_-|^2 - \left(\frac{\hbar}{c}\omega\right) + 2\frac{\hbar}{c}\omega|\mathbf{p}_+| \cos\Theta_+, \tag{102}$$

$$\Delta_2^{(p)} \quad := \quad 2\frac{\hbar}{c}\omega|\mathbf{p}_i| - 2|\mathbf{p}_+||\mathbf{p}_-| \cos\Theta_+. \tag{103}$$

4. Discussion

4.1. Bremsstrahlung

4.1.1. Angular distribution of Bremsstrahlung

If electrons are scattered at nuclei, they can produce hard Bremsstrahlung photons with frequency ω and direction Θ_i relative to the direction of the electrons.

Figure 2 shows the doubly differential cross section (60) for Bremsstrahlung for several electron and photon energies. At first, the probability for generating photons decreases with increasing photon energy for fixed electron energy. This can be understood easily by applying (81). As can be seen there, the doubly differential cross section grows linearly in the momentum of the electron in the final state which is equivalent to

$$\frac{d^2\sigma}{d\omega d\Omega_i} \sim |\mathbf{p}_f| \tag{104}$$

for high photon energies. So, if all kinetic energy is transferred from the electron onto the photon, the final momentum $|\mathbf{p}_f|$ vanishes, and thus

$$\frac{d^2\sigma}{d\omega d\Omega_i} \to 0. \tag{105}$$

For nonrelativistic electron and photon energies the scattering angle tends to be mainly equally distributed, i.e. the photons do not have a preference for a particular direction. When the photon energy increases, photons are mainly emitted in forward direction, but the ratio between forward and backward scattering is at least three orders of magnitude lower than for a relativistic electron. This case belongs to the classical case where the velocity is small compared to the speed of light. Namely, it is $v/c|_{E_{kin,i}=10\mathrm{keV}} \approx 0.20$ and non-relativistic equations will be enough to describe these phenomena. In the relativistic case ($v/c|_{E_{kin,i}=1\mathrm{MeV}} \approx 0.94$ and $v/c|_{E_{kin,i}=100\mathrm{MeV}} \approx 0.99999$) the differential cross section becomes more and more anisotropic. Forward scattering is preferred to backward scattering although the maximal cross section does not lie precisely at $\Theta_i = 0$ as can be seen in figure 2 c). But the more the electron energy increases the more the maximum wanders to smaller angles, for example, it seems in figure 2 d) that the maximal emission is indeed for Θ_i=0. As mentioned in section 2.4 and in Appendix B, formula (61) cannot be evaluated directly at $\Theta_i = 0$. However, for this purpose, we

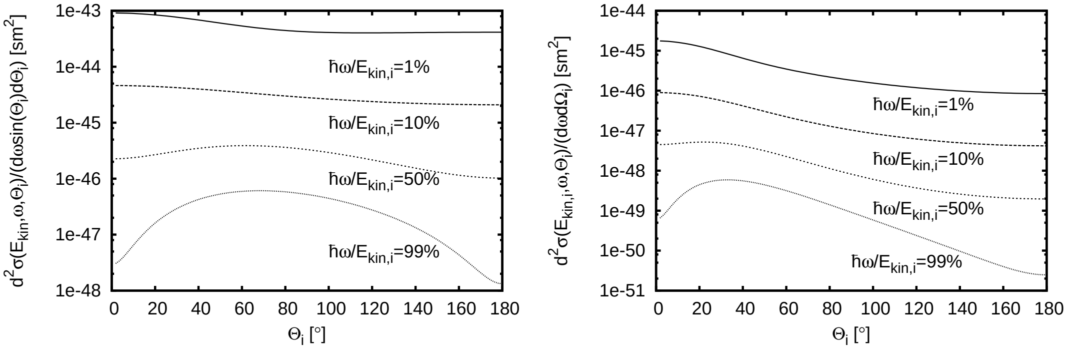

a) $E_{kin,i} = 10$ keV

b) $E_{kin,i} = 150$ keV

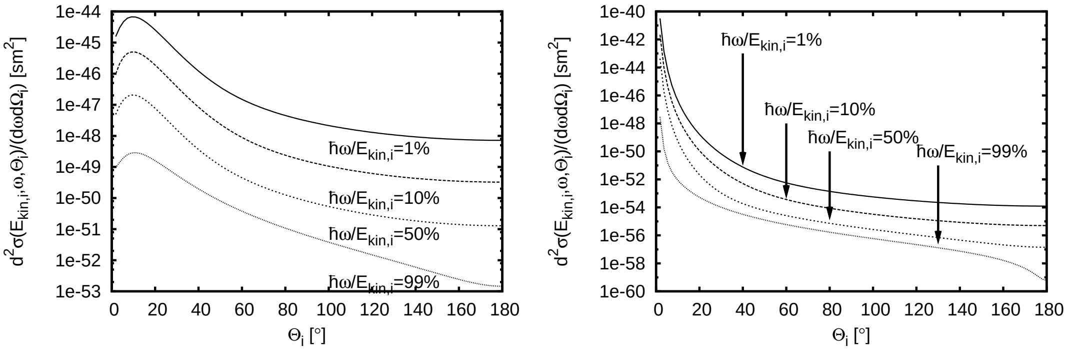

c) $E_{kin,i} = 1$ MeV

d) $E_{kin,i} = 100$ MeV

Figure 2: The doubly differential cross section $d^2\sigma/(d\omega d\Omega_i)(E_{kin,i}, \omega, \Theta_i)$ for Bremsstrahlung ($Z = 7$) versus the scattering angle Θ_i between emitted photon and incident electron. The electron energies are a) $E_{kin,i} = 10$ keV, b) $E_{kin,i} = 150$ keV, c) $E_{kin,i} = 1$ MeV and d) $E_{kin,i} = 100$ MeV. In each plot the the photon energy $\hbar\omega$ amounts to $1\%, 10\%, 50\%$ and 95% of the kinetic energy of the incident electron.

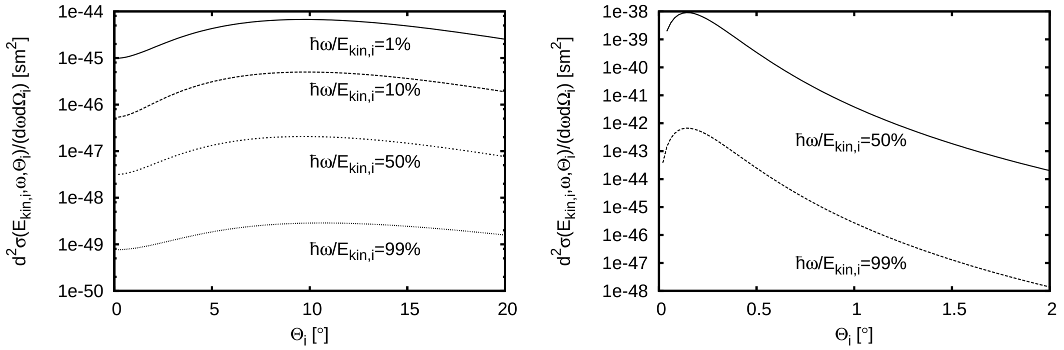

a) $E_{kin,i} = 1$ MeV b) $E_{kin,i} = 100$ MeV

Figure 3: The doubly differential cross section $d^2\sigma/(d\omega d\Omega_i)$ as in figure 2 for a smaller angular range

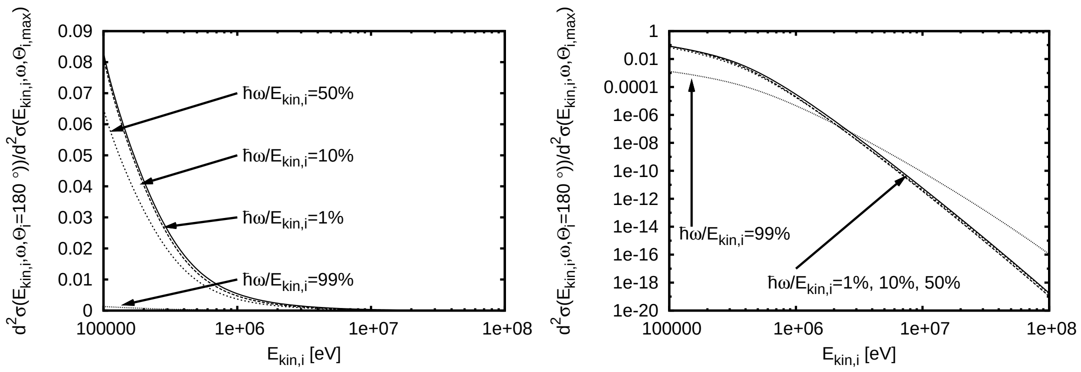

a) b)

Figure 4: The ratio between the doubly differential cross section for backward scattering ($\Theta_i = 180°$) $d^2\sigma(E_{kin,i}, \omega, \Theta_i = 180°)/(d\omega d\Omega_i)$ and the maximum of this cross section $\max\left(d^2\sigma(E_{kin,i}, \omega, \Theta_i)/(d\omega d\Omega_i)\right)$ vs. the kinetic energy of the incident electron for different ratios between photon and electron energies in a a) linear and b) logarithmic scale for $Z = 7$.

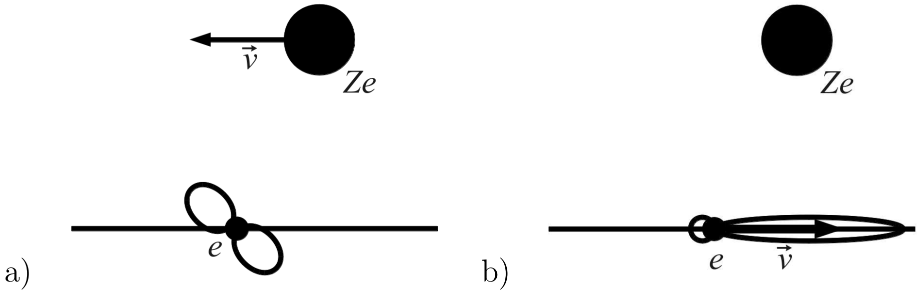

Figure 5: a) In the rest frame of the electron where the nucleus is moving instead radiation is emitted isotropically with a small-angle deflection. b) If, however, one transforms the situation into the rest frame of the nucleus where the electron is moving, most of the radiation is emitted in forward direction relative to the direction of the electron.

derived (74) which is valid for $\Theta_i = 0$ and $\Theta_i = \pi$. Figure 3 shows again (60) for two relativistic electron and different photon energies but for a smaller range of angles. It shows in more detail that the angle of maximal scattering is small, but not 0.

Figure 4 shows the ratio between the cross section for backward scattering and forward scattering. It can be clearly seen that the tendency for backward scattering decreases for increasing electron energy. The lower the electron energy becomes, the more forward and backward scattering become similar and in general, the scattering tends to be isotropic. Only for ratios between photon energies and electron energies close to 1, forward scattering is preferred for the whole range of energies, but still decreases with increasing electron energies.

4.1.2. Relativistic transformation

The tendency of forward scattering in the case of relativistic incident electrons can be understood by applying the laws of relativistic transformations. Imagine a non-quantum field theoretical description of Bremsstrahlung (Jackson, 1975). If one regards an inertial system in which the incident particle is at rest (Fig. 5 a)), radiation is emitted isotropically with a small-angle deflection. If the physical laws for this process are relativistically transformed into the laboratory system where the nucleus is at rest and the electron moving, most of the radiation is emitted in forward direction relative to the electron direction (Fig. 5 b)). Because this transformation is valid for a non-quantum field theoretical, relativistic electron, it must also be true for a

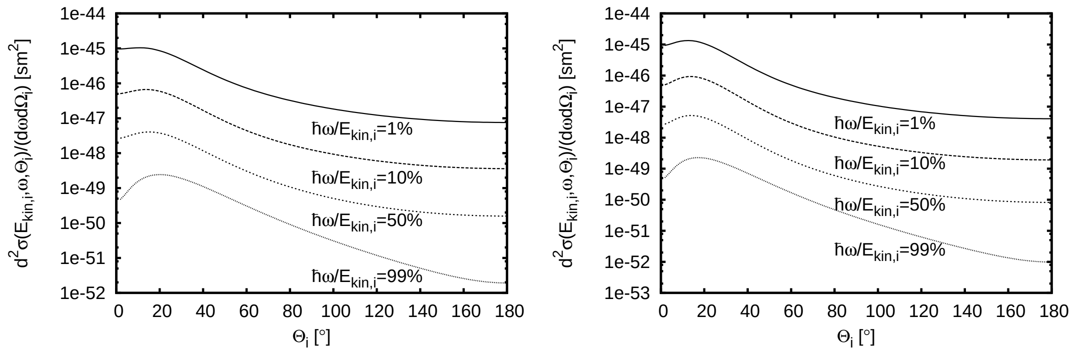

a) $E_{kin,i} = 400$ keV

b) $E_{kin,i} = m_e c^2 \approx 511$ keV

Figure 6: The doubly differential cross section $d^2\sigma/(d\omega d\Omega_i)(E_{kin,i}, \omega, \Theta_i)$ for Bremsstrahlung ($Z = 7$) versus the scattering angle Θ_i between emitted photon and incident electron. The electron energies are a) $E_{kin,i} = 400$ keV, b) $E_{kin,i} \approx 511$ keV. In each plot the the photon energy $\hbar\omega$ amounts to $1\%, 10\%, 50\%$ and 95% of the kinetic energy of the incident electron.

relativistic quantum theoretical description, therefore we see that the forward scattering of photons can simply be explained as a result of the relativistic transformation.

The forward scattering can moreover be understood by using the conservation laws of energy and momentum. They predict that photons have to be scattered in forward direction if electron and photon energy are high. The interested reader is referred to Appendix G.

Although figure 2 shows that the maxima of the doubly differential cross section form with increasing electron energy, it is difficult to determine in these plots when these maxima really start to be generated clearly. Figure 6 shows the doubly differential cross section in dependence of the incident electron energy for $E_{kin,i} = 400$ keV and $E_{kin,i} \approx 511$ keV when the kinetic energy is equal to the rest energy. For 400 keV and for $\hbar\omega/E_{kin,i} = 0.01$ the cross section for forward scattering is already two orders of magnitude larger than for backward scattering, but a clear maximum cannot be seen. However, for the same kinetic energy, but for $\hbar\omega/E_{kin,i} = 0.95$ there is already a clear maximum formed. But if the kinetic energy grows up to 511 keV which is equal to the rest energy of the electron, there is even a maximum for $\hbar\omega = 0.01 E_{kin,i}$. This can be expected due to the relativistic transformation. If $E_{kin,i} \ll m_e c^2$, then the photon emission is relatively isotropic. But if the kinetic energy is approximately equal to the rest energy of the electron, relativistic laws are valid. Especially for $E_{kin,i} = m_e c^2$

$$\frac{v}{c} = \frac{\sqrt{3}}{2} \approx 87\%, \tag{106}$$

therefore the electron has to be treated relativistically and clear maxima close to $\Theta_i = 0$ form for every possible photon energy.

4.1.3. Dependence on the energy of the emitted photon

Figure 2 shows that for both slow and relativistic electrons the doubly differentical cross section also varies with the photon energy for fixed electron energies. For fixed electron energy, low er photon energies are more likely. Moreover, the probability of photon generation is larger for low energetic electrons, but this is only true on average. Figure 7 shows the doubly differential cross section in another way. Now the photon energy is fixed and the electron energy differs within one plot. For all cases it is more likely that low energetic electrons create photons than relativistic electrons do. This can be understood if one goes one step back to the triply differential cross section (1). Considering that due to (2) and (9) $|\mathbf{p}_i| \sim E_i$ and $|\mathbf{q}|^2 \sim |\mathbf{p}_i|^2 \sim E_i^2$, (1) behaves like

$$\frac{d^4\sigma}{d\omega d\Omega_i d\Omega_f d\Phi} \sim \frac{1}{E_i^4}, \tag{107}$$

therefore (1) decreases if the energy of the incident electron increases. And because of the fact that integration preserves monotony, the doubly differential cross section (60) has to decrease for increasing electron energy as well. But for small angles, i.e. for forward emission of photons, the probability rapidly increases for relativistic electrons and exceeds the probability at small electron energies.

4.1.4. The most probable scattering angle

Figure 2 also shows that the angle for which maximal scattering takes place, is rather independent of the photon energy. Hence, one can use (81) to determine a formula for that scattering angle. Actually this derivation leads to a quartic equation which can, however, be approximated for small angles, i.e. $\Theta_i \lesssim 20°$, through a quadratic equation. The reader is referred

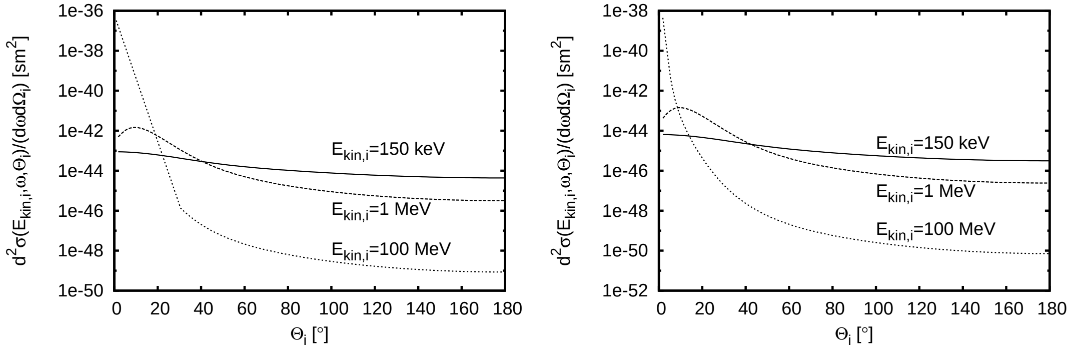

a) $\hbar\omega = 50$ eV   b) $\hbar\omega = 500$ eV

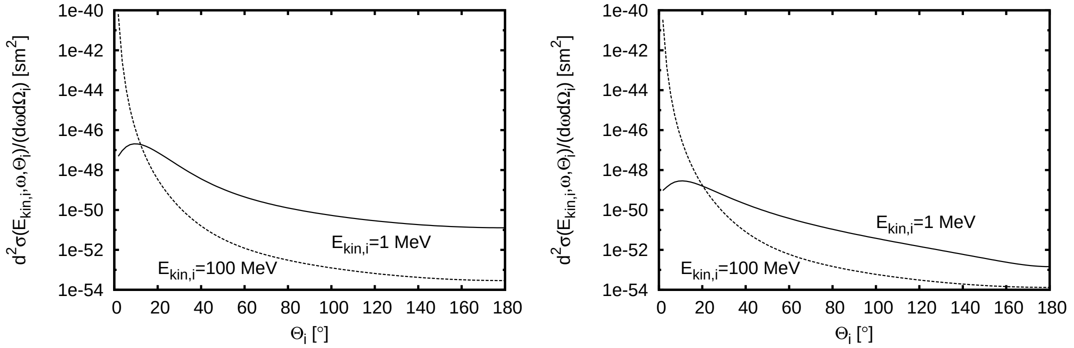

c) $\hbar\omega = 500$ keV   d) $\hbar\omega = 950$ keV

Figure 7: The doubly differential cross section $d^2\sigma/(d\omega d\Omega_i)(E_{kin,i},\omega,\Theta_i)$ for Bremsstrahlung ($Z = 7$) vs. the scattering angle Θ_i for several electron and photon energies. In each panel the photon energy $\hbar\omega$ is fixed and the cross section is plotted for various kinetic energies of the incident electron.

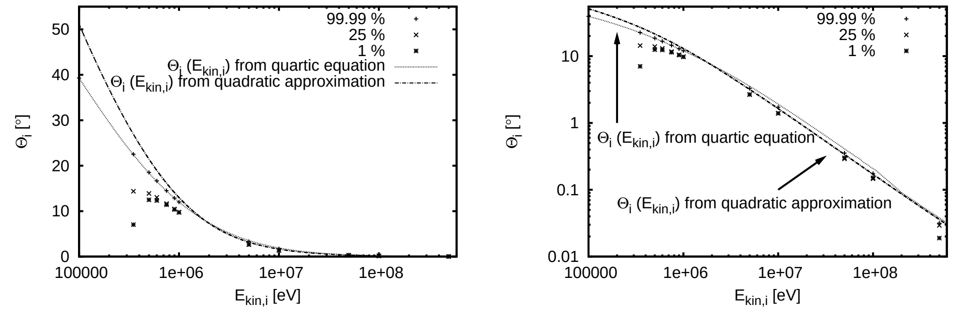

a)

b)

Figure 8: Θ_i for maximal scattering vs. incident electron energy in a a) semilog and b) loglog plot for $Z = 7$. Besides (108) for $\hbar\omega = 0.9999 E_{kin,i}$, the exact solution of the quartic equation and various data for different $\hbar\omega / E_{kin,i}$ are shown.

to Appendix H for the detailed calculation. The solution of the quadratic equation reads

$$\Theta_i = \sqrt{\frac{-\frac{\delta_0}{\hbar\omega}(4E_f^2 + \delta_0 c^2) - \frac{2\delta_0 \hbar\omega}{E_f}(E_i - c|\mathbf{p}_i|)}{2\frac{|\mathbf{p}_i|}{c}\left[4E_f^2 + \delta_0 c^2 + \frac{2\hbar^2\omega^2}{E_f}(E_i - c|\mathbf{p}_i|)\right] - |\mathbf{p}_i|\delta_0 c - \frac{\hbar\omega}{E_f} c|\mathbf{p}_i|\delta_0}} \tag{108}$$

with

$$\delta_0 := -|\mathbf{p}_i|^2 - \left(\frac{\hbar}{c}\omega\right)^2 + 2\frac{\hbar}{c}\omega|\mathbf{p}_i|, \tag{109}$$

$\hbar\omega \to E_{kin,i}$, e.g. $\hbar\omega = 0.9999 E_{kin,i}$ and

$$p_i = \sqrt{E_{kin,i}\left(\frac{E_{kin,i}}{c^2} + 2m_e\right)}. \tag{110}$$

Figure 8 shows (108) and manually extracted values for Θ_i for different photon energies. It shows much better than figure 2 that Θ_i is rather independent of the photon energy for relativistic electron energies. Besides (108), the solution of the quartic equation, is shown. Moreover, it shows that (108) gives a good approximation for those angles Θ_i for which scattering is maximal. Actually, we see that the exact solution describes the angle for maximal scattering better, especially for low energies, but for high energies both curves fit very well.

By inserting $E_{kin,i} = \hbar\omega/0.9999$ into (108) one obtains a formula which relates the photon energy to the most probable scattering angle.

4.2. Pair production

4.2.1. Basic properties of pair production

We now proceed from Bremsstrahlung to pair production. One photon with energy $\hbar\omega$ creates two particles, namely an electron and a positron, both with rest energy $m_e c^2$. Therefore

$$E_{kin,-} + E_{kin,+} = \hbar\omega - 2m_e c^2 \tag{111}$$

follows for the kinetic energies of these two particles. Thus the photon energy has to be $\hbar\omega \geq 2m_e c^2 \approx 1.022$ MeV for pair production and the kinetic energy of the particles is bounded as $E_{kin,\pm} \leq \hbar\omega - 2m_e c^2$. Figure 9 shows the doubly differential cross section (94) for different photon and positron energies. Forward scattering is preferred, but there is almost no case now of more isotropic scattering . This results from the fact that the incident particle is a photon and these have always to be treated relativistically. For very highly energetic photons, e.g. 50 MeV and 100 MeV, there are clear maxima for forward scattering. Additionally positrons with higher energies are less probable than positrons with lower energies which is the same as for photons emitted due to Bremsstrahlung. For energies $\hbar\omega < 50$ MeV , however, the maxima are $> 5^\circ$, but forward scattering is still preferred. However, there is a new phenomenon which has not occurred for Bremsstrahlung or for highly energetic pair production. The production of Bremsstrahlung photons with higher energies has always been more probable than for small energies. But figure 9 also shows that the probability for highly energetic positrons can exceed the probability for lowly energetic positrons, at least for small angles. Figure 10 shows (94) for fixed positron and different photon energies. Again positrons which are generated with high velocities prefer to be scattered forward while this tendency vanishes if the positron energy is very low. This can be traced back to the relativistic behaviour again. If a positron is very energetic, it has to be treated relativistically and the relativistic transformation leads to forward scattering (this is the same explanation as for Bremsstrahlung). We also see that the creation of positrons is more likely for highly energetic photons.

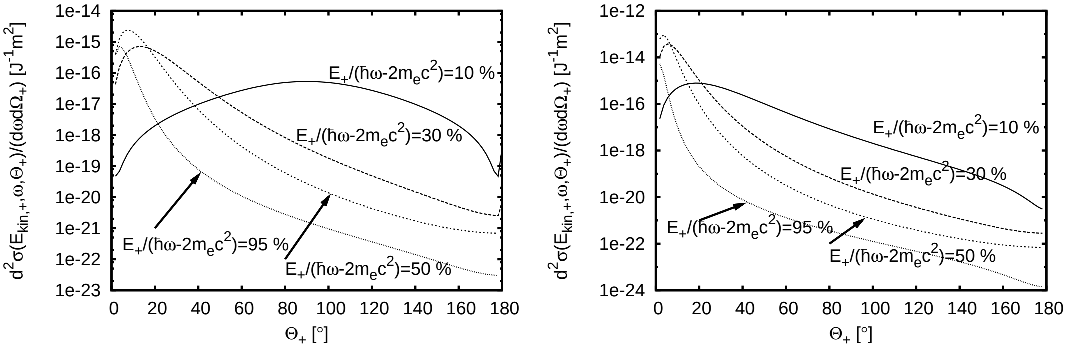

a) $\hbar\omega = 5$ MeV b) $\hbar\omega = 10$ MeV

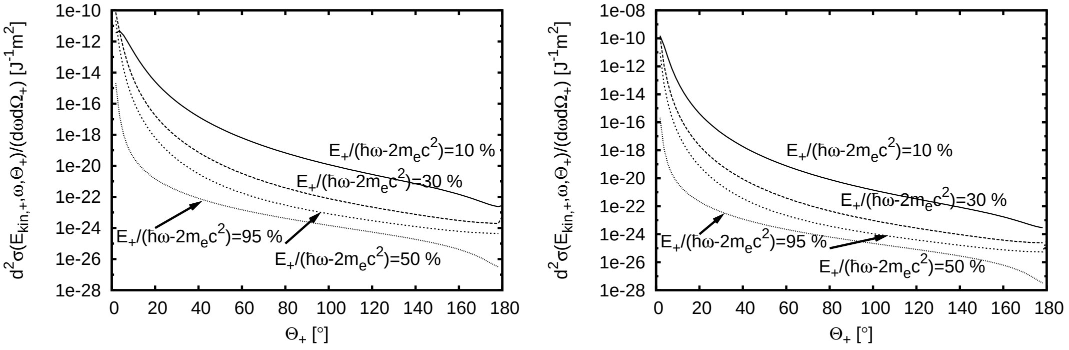

c) $\hbar\omega = 50$ MeV d) $\hbar\omega = 100$ MeV

Figure 9: Doubly differential cross section $d^2\sigma(E_+, \omega, \Theta_+)/(dE_+ d\Omega_+)$ vs. Θ_+ as an angle between incident photon and created positron for $Z = 7$: The cross section is shown for a) $\hbar\omega = 5$ MeV, b) $\hbar\omega = 10$ MeV, c) $\hbar\omega = 50$ MeV and d) $\hbar\omega = 100$ MeV. In each panel different positron energies E_+ relative to the available photon energy $\hbar\omega - 2m_e c^2$ are plotted.

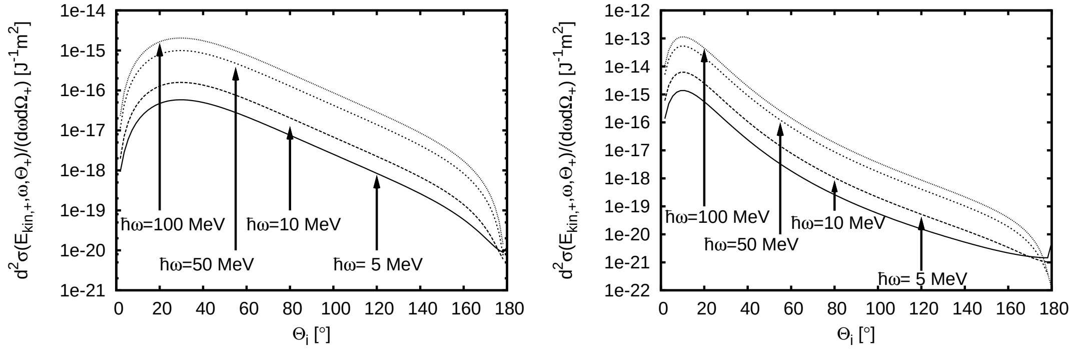

a) $E_{kin,+} = 150$ keV b) $E_{kin,+} = 1$ MeV

Figure 10: Doubly differential cross section $d^2\sigma(E_+, \omega, \Theta_+)/(dE_+ d\Omega_+)$ vs. Θ_+ as an angle between incident photon and created positron for $Z = 7$: The cross section is shown for a) $E_{kin,+} = 150$ keV and b) $E_{kin,+} = 1$ MeV. In each panel the photon energies are $\hbar\omega = 5$ MeV, 10 MeV, 50 MeV and 100 MeV.

4.2.2. The most probable scattering angle

As for Bremsstrahlung one can get a simple formula for the preferred direction. Performing the same calculation as for Bremsstrahlung one obtains

$$\begin{aligned}\Theta_+ &= \Bigg[\Big(-\frac{\delta_0^{(p)}}{\hbar\omega}(-4E_-^2 - \delta_0^{(p)}c^2) - \frac{2\delta_0^{(p)}\hbar\omega}{E_-}(E_+ - c|\mathbf{p}_+|)\Big) \\ &\times \Big(2\frac{|\mathbf{p}_+|}{c}\Big[-4E_-^2 - \delta_0^{(p)}c^2 + \frac{2\hbar^2\omega^2}{E_-}(E_+ - c|\mathbf{p}_+|)\Big] - |\mathbf{p}_+|\delta_0^{(p)}c \\ &- \frac{\hbar\omega}{E_-}c|\mathbf{p}_+|\delta_0^{(p)}\Big)^{-1}\Bigg]^{\frac{1}{2}} \end{aligned} \tag{112}$$

with

$$\delta^{(p)} := -|\mathbf{p}_+|^2 - \left(\frac{\hbar}{c}\omega\right)^2 + 2|\mathbf{p}_+|\frac{\hbar}{c}\omega \tag{113}$$

and

$$\frac{E_+ - m_e c^2}{\hbar\omega - 2m_e c^2} \approx 1. \tag{114}$$

Figure 11 shows that (112) is a good approximation for Θ_+ for high photon

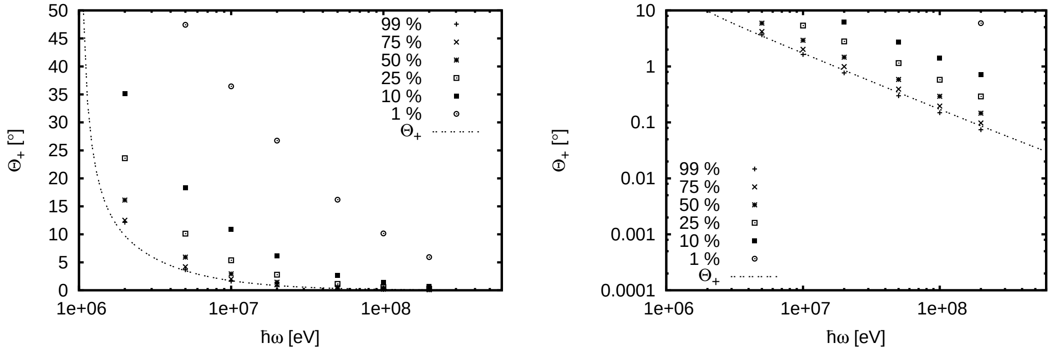

a) b)

Figure 11: Θ_+ for maximal scattering vs. incident photon energy in a a) semilog and b) loglog plot for $Z = 7$. Besides (112) for $E_{kin,+}/(\hbar\omega - 2m_ec^2) = 0.9999$ various data for different $E_{kin,+}/(\hbar\omega - 2m_ec^2)$ are shown.

energies and high ratios between photon and positron energy. The smaller the ratio between photon and positron energy, however, is, the worse (112) becomes for low photon energies. If the photon energy is larger than 50 MeV, relativistic positrons are created; therefore forward scattering takes place and Θ_+ can be calculated with (112).

5. Conclusion

We have reviewed literature relevant for Bremsstrahlung in Terrestrial gamma-ray flashes (TGFs) (Bethe and Heitler, 1934; Heitler, 1944; Elwert and Haug, 1969; Seltzer and Berger, 1985; Shaffer et al., 1996; Agostinelle et al., 2003). Focussing on atomic numbers $Z = 7$ (nitrogen) and $Z = 8$ (oxygen) and an energy range of 1 keV to 1 GeV, no good parametrization of an energy resolved angular distribution in the form of doubly differential cross section is available. The theory of Bethe and Heitler covers this energy range for $Z = 7, 8$, but it parameterizes the direction of the scattered electron as well; therefore we integrated their triply differential cross section to obtain the correct energy resolved angular distribution for Bremsstrahlung and pair production. Other authors (Lehtinen, 2000; Dwyer, 2007; Carlson et al., 2009, 2010) used different approaches, as discussed in the introduction. They use singly or triply differential cross sections which do not give a direct relation between the photon energy and the direction of the photon relative to the motion of the electron. As positrons are created within a thundercloud as well (Briggs et al., 2010), we used a symmetry between the production of Bremsstrahlung and the creation of an electron-positron pair both in the field of a nucleus to obtain a cross section which relates the energy of the created positron with its direction.

We have seen that emitted Bremsstrahlung photons are mainly released in forward direction if the electron which interacts with the nucleus has such a high energy that it has to be treated relativistically. For lower energies scattering tends to be more isotropic. For the case that almost all kinetic energy of the incident electron is transformed into photon energy, we derived an approximation for the most probable photon emission angle as a function of the incident electron energy and of the photon energy. The expression is valid for all ratios of photon over electron energy if the electron motion is relativistic. So, when photons have been created within a thundercloud or discharge, they are mainly scattered in forward direction as long as the electrons move relativistically, i.e. if their kinetic energy is at least as large as their rest energy.

Similar results hold for pair production. Next to the doubly differential cross section we derived a simple approximation for the most probable positron emission angle for the case that the photon energy is larger than 10 MeV (for ratios between the kinetic energy of the positron and available photon energy down to 25%) or than 100 MeV (for ratios lower than 25%).

We have seen that for very highly energetic photons that almost all positrons are scattered in forward direction. If, however, the photon energy decreases, the probability of forward scattering decreases as well. Instead the maximal cross section can be found at $\Theta_+ \approx 90^\circ$ for low ratios between E_+ and $\hbar\omega - 2m_e c^2$ and is, beyond that, symmetric to this angle.

Our analytical results for the doubly differential cross-sections for Bremsstrahlung and pair production are also supplied in the form of two functions written in C++. In this form the functions can be implemented into Monte Carlo codes simulating energetic processes like the production of gamma-rays or electron positron pairs in thunderstorms.

Acknowledgements: We dedicate this article to the memory of Davis D. Sentman. He was a great inspiration and discussion partner in the summer of 2011 when C.K. worked on this project, and he was an invaluable colleague and co-organizer for U.E. for many years. We acknowledge fruitful and motivating discussions with Brant Carlsson. C.K. acknowledges financial support by STW-project 10757, where Stichting Technische Wetenschappen (STW) is part of The Netherlands' Organization for Scientific Research NWO.

Appendix A. The residual theorem to calculate integrals with trigonometric functions

In this appendix the method how to calculate integrals of the form

$$\int_0^{2\pi} R(\cos\Phi, \sin\Phi) d\Phi \tag{A.1}$$

shall be discussed where $R(x, y) : \mathbb{R}^2 \setminus \{x, y \in \mathbb{R} | y = \pm\sqrt{1 - x^2}\} \to \mathbb{R}$ is a rational function without poles on the unit circle $x^2 + y^2 = 1$. But before explaining this method let's briefly review some general facts about residua.

Appendix A.1. The residual theorem

Let $f : \mathbb{C} \supset I \to \mathbb{C}, z \mapsto f(z)$, be a holomorphic function and $\Gamma : [a, b] \to \mathbb{C}, t \mapsto \Gamma(t)$, a closed curve in the complex plane. Then one can calculate complex curve integrals via

$$\int_\Gamma f(z)dz = 2\pi i \sum_j \operatorname{Res}(f, z_j) \tag{A.2}$$

where the sum has to be taken over all poles z_j of f and complex curve integrals are defined as

$$\int_\Gamma f(z)dz := \int_a^b f(\Gamma(t)) \cdot \frac{d\Gamma}{dt}(t)dt. \tag{A.3}$$

The residuum of a pole z_j can be calculated via

$$\operatorname{Res}(f, z_j) = \frac{1}{(n-1)!} \lim_{z \to z_j} \frac{d^{n-1}}{dz^{n-1}} \Big[(z - z_j)f(z)\Big] \tag{A.4}$$

where n denotes the order of the pole.

Appendix A.2. Integral with trigonometric functions

With the help of the (A.2) one can simply perform the integration of (A.1). For that purpose define

$$f(z) := \frac{1}{iz} R\left(\frac{1}{2}\left(z + \frac{1}{z}\right), \frac{1}{2i}\left(z - \frac{1}{z}\right)\right) \tag{A.5}$$

and choose the unit circle

$$\Gamma(t) = e^{it}, t \in [0, 2\pi] \tag{A.6}$$

as closed curve; hence (A.3) becomes

$$\begin{aligned}
\int\limits_{\Gamma} f(z)dz &= \int\limits_{0}^{2\pi} \frac{1}{ie^{it}} R\left(\frac{1}{2}\left(e^{it} + e^{-it}\right), \frac{1}{2i}\left(e^{it} - e^{-it}\right)\right) ie^{it} dt && \text{(A.7)} \\
&= \int\limits_{0}^{2\pi} R\left(\frac{1}{2}\left(e^{it} + e^{-it}\right), \frac{1}{2i}\left(e^{it} - e^{-it}\right)\right) dt && \text{(A.8)} \\
&= \int\limits_{0}^{2\pi} R(\cos t, \sin t) dt && \text{(A.9)}
\end{aligned}$$

where the identities $\cos t = 1/2\left(e^{it} + e^{-it}\right)$ and $\sin t = 1/(2i)\left(e^{it} - e^{-it}\right)$ were used in the last step.

Finally with (A.2) and (A.9) one gets a simple formula to calculate (A.1):

$$\int\limits_{0}^{2\pi} R(\cos\Phi, \sin\Phi) d\Phi = 2\pi i \sum_{|z|<1} \mathrm{Res}(f, z) \tag{A.10}$$

with f being defined in (A.5).

Appendix B. The doubly differential cross section for $\boldsymbol{\Theta_i = 0}$ and $\boldsymbol{\Theta_i = \pi}$

In order to get (74) from (60) it is rather straight forward to set $\Theta_i = 0$ or $\Theta_i = \pi$. Especially it is

$$\begin{aligned}
\Delta_1(\Theta_i = 0, \pi) &= \tilde{\Delta}_1, && \text{(B.1)} \\
\Delta_2(\Theta_i = 0, \pi) &= \tilde{\Delta}_2. && \text{(B.2)}
\end{aligned}$$

But there is one case which should be considered a bit more thoroughly.

This regards the logarithm in (61). For $\Theta_i = \pi$ it is $\Delta_2(\Theta = \pi) = \tilde{\Delta}_2 =$

$-2p_f(\hbar/c\,\omega + p_i) < 0$; thus $|\tilde{\Delta}_2| = -\tilde{\Delta}_2$ and

$$\left.\frac{\ln\left(\frac{\Delta_2^2+4p_i^2p_f^2\sin^2\Theta_i-\sqrt{\Delta_2^2+4p_i^2p_f^2\sin^2\Theta_i}(\Delta_1+\Delta_2)+\Delta_1\Delta_2}{-\Delta_2^2-4p_i^2p_f^2\sin^2\Theta_i-\sqrt{\Delta_2^2+4p_i^2p_f^2\sin^2\Theta_i}(\Delta_1-\Delta_2)+\Delta_1\Delta_2}\right)}{\sqrt{\Delta_2^2+4p_i^2p_f^2\sin^2\Theta_i}}\right|_{\Theta_i=\pi} \tag{B.3}$$

$$= \frac{1}{|\tilde{\Delta}_2|}\ln\left(\frac{\tilde{\Delta}_2^2-|\tilde{\Delta}_2|(\tilde{\Delta}_1+\tilde{\Delta}_2)+\tilde{\Delta}_1\tilde{\Delta}_2}{-\widetilde{\Delta_2}^{\,2}-|\tilde{\Delta}_2|(\tilde{\Delta}_1-\tilde{\Delta}_2)+\tilde{\Delta}_1\tilde{\Delta}_2}\right) \tag{B.4}$$

$$= -\frac{1}{\tilde{\Delta}_2}\ln\left(\frac{\tilde{\Delta}_1+\tilde{\Delta}_2}{\tilde{\Delta}_1-\tilde{\Delta}_2}\right) \tag{B.5}$$

which is a very simple calculation. However, for $\Theta_i = 0$ it is $\Delta_2(\Theta_i = 0) = \tilde{\Delta}_2 = -2p_f(\hbar/c\,\omega - p_i)$ which can be both negative or positive depending on values of p_i and $\hbar/c\,\omega$ If $\tilde{\Delta}_2 < 0$ then equations (B.3) - (B.5) are valid again. If $\tilde{\Delta}_2 > 0$, however, it follows for the argument of the logarithm

$$\left.\frac{\Delta_2^2+4p_i^2p_f^2\sin^2\Theta_i-\sqrt{\Delta_2^2+4p_i^2p_f^2\sin^2\Theta_i}(\Delta_1+\Delta_2)+\Delta_1\Delta_2}{-\Delta_2^2-4p_i^2p_f^2\sin^2\Theta_i-\sqrt{\Delta_2^2+4p_i^2p_f^2\sin^2\Theta_i}(\Delta_1-\Delta_2)+\Delta_1\Delta_2}\right|_{\Theta_i=0} \tag{B.6}$$

$$= \frac{\tilde{\Delta}_2^2-\tilde{\Delta}_2(\tilde{\Delta}_1+\tilde{\Delta}_2)+\tilde{\Delta}_1\tilde{\Delta}_2}{-\tilde{\Delta}_2^2-\tilde{\Delta}_2(\tilde{\Delta}_1-\tilde{\Delta}_2)+\tilde{\Delta}_1\tilde{\Delta}_2} = \frac{0}{0}. \tag{B.7}$$

Hence it is necessary to use the rule of L'Hospital:

$$\lim_{\Theta_i\to 0}\frac{\Delta_2^2+4p_i^2p_f^2\sin^2\Theta_i-\sqrt{\Delta_2^2+4p_i^2p_f^2\sin^2\Theta_i}(\Delta_1+\Delta_2)+\Delta_1\Delta_2}{-\Delta_2^2-4p_i^2p_f^2\sin^2\Theta_i-\sqrt{\Delta_2^2+4p_i^2p_f^2\sin^2\Theta_i}(\Delta_1-\Delta_2)+\Delta_1\Delta_2} \tag{B.8}$$

$$= \lim_{\Theta_i\to 0}\frac{8p_i^2p_f^2\sin\Theta_i\cos\Theta_i-\frac{\Delta_1+\Delta_2}{2\sqrt{\Delta_2^2+4p_i^2p_f^2\sin^2\Theta_i}}\cdot 8p_i^2p_f^2\sin\Theta_i\cos\Theta_i}{-8p_i^2p_f^2\sin\Theta_i\cos\Theta_i-\frac{\Delta_1-\Delta_2}{2\sqrt{\Delta_2^2+4p_i^2p_f^2\sin^2\Theta_i}}\cdot 8p_i^2p_f^2\sin\Theta_i\cos\Theta_i} \tag{B.9}$$

$$= \ln\left(\frac{\tilde{\Delta}_1-\tilde{\Delta}_2}{\tilde{\Delta}_1+\tilde{\Delta}_2}\right). \tag{B.10}$$

With (B.10) the whole limit yields

$$\left.\frac{\ln\left(\frac{\Delta_2^2+4p_i^2p_f^2\sin^2\Theta_i-\sqrt{\Delta_2^2+4p_i^2p_f^2\sin^2\Theta_i}(\Delta_1+\Delta_2)+\Delta_1\Delta_2}{-\Delta_2^2-4p_i^2p_f^2\sin^2\Theta_i-\sqrt{\Delta_2^2+4p_i^2p_f^2\sin^2\Theta_i}(\Delta_1-\Delta_2)+\Delta_1\Delta_2}\right)}{\sqrt{\Delta_2^2+4p_i^2p_f^2\sin^2\Theta_i}}\right|_{\Theta_i=0} \tag{B.11}$$

$$= \frac{1}{\tilde{\Delta}_2}\ln\left(\frac{\tilde{\Delta}_1-\tilde{\Delta}_2}{\tilde{\Delta}_1+\tilde{\Delta}_2}\right) = -\frac{1}{\tilde{\Delta}_2}\ln\left(\frac{\tilde{\Delta}_1+\tilde{\Delta}_2}{\tilde{\Delta}_1-\tilde{\Delta}_2}\right) \tag{B.12}$$

which is and has to be identical with (B.5). So in both cases, $\tilde{\Delta}_2 > 0$ and $\tilde{\Delta}_2 < 0$, (B.5,B.12) are generated by setting $\Theta_i = 0, \pi$; therefore one does not have to distinguish between the these cases in (74).

But it is of importance to mention that due to (B.7) one can get numerical problems if one only implements (60) and wants to calculate the doubly differential cross section for $\Theta_i = 0$. Thus it is useful to distinguish for $\Theta_i \neq 0$ and $\Theta_i = 0$ and to use (74) instead for the latter case.

For the rest of limiting forward and/or backward scattering it is, however, straight forward to insert $\Theta_i = 0, \pi$ and thus can deduce (74) from (60) with the additional help of (B.10).

Appendix C. The doubly differential cross section for $\hbar\omega \to E_{kin,i}$

There are three contributions from (60) which lead to (81) in the limit $\hbar\omega \to E_{kin,i} \Leftrightarrow |\mathbf{p}_f| \to 0$:

$$\iota_1 = \frac{16\pi E_f^2 p_i^2 \sin^2\Theta_i A}{(E_i - cp_i\cos\Theta_i)^2(\Delta_1^2-\Delta_2^2-4p_i^2p_f^2\sin^2\Theta_i)}, \tag{C.1}$$

$$\begin{aligned}
\iota_2 &= -\frac{2\pi A p_i^2 c^2 \sin^2\Theta_i}{(E_i - cp_i\cos\Theta_i)^2}\frac{1}{\sqrt{\Delta_2^2+4p_i^2p_f^2\sin^2\Theta_i}} \\
&\times \ln\left(\frac{\Delta_2^2+4p_i^2p_f^2\sin^2\Theta_i-\sqrt{\Delta_2^2+4p_i^2p_f^2\sin^2\Theta_i}(\Delta_1+\Delta_2)+\Delta_1\Delta_2}{-\Delta_2^2-4p_i^2p_f^2\sin^2\Theta_i-\sqrt{\Delta_2^2+4p_i^2p_f^2\sin^2\Theta_i}(\Delta_1-\Delta_2)+\Delta_1\Delta_2}\right),
\end{aligned} \tag{C.2}$$

$$\begin{aligned}
\iota_3 &= -\frac{4\pi\hbar^2\omega^2p_i^2\sin^2\Theta_i A}{E_i - cp_i\cos\Theta_i}\Bigg[-\frac{2\Delta_1\Delta_2p_fc+2\Delta_2^2E_f+8p_i^2p_f^2\sin^2\Theta_iE_f}{(-\Delta_2^2+\Delta_1^2-4p_i^2p_f^2\sin^2\Theta_i)((\Delta_2E_f+\Delta_1p_fc)^2+4m^2c^4p_i^2p_f^2\sin^2\Theta_i)} \\
&+ \frac{p_fc(\Delta_2E_f+\Delta_1p_fc)}{\sqrt{((\Delta_2E_f+\Delta_1p_fc)^2+4m^2c^4p_i^2p_f^2\sin^2\Theta_i)^3}} \\
&\times \ln\Bigg(\bigg((E_f+p_fc)(4p_i^2p_f^2\sin^2\Theta_i(E_f-p_fc)+(\Delta_1+\Delta_2)((\Delta_2E_f+\Delta_1p_fc) \\
&- \sqrt{(\Delta_2E_f+\Delta_1p_fc)^2+4m^2c^4p_i^2p_f^2\sin^2\Theta_i}))\bigg)\bigg((E_f-p_fc)(4p_i^2p_f^2\sin^2\Theta_i(-E_f-p_fc) \\
&+ (\Delta_1-\Delta_2)((\Delta_2E_f+\Delta_1p_fc)-\sqrt{(\Delta_2E_f+\Delta_1p_fc)^2+4m^2c^4p_i^2p_f^2\sin^2\Theta_i}))\bigg)^{-1}\Bigg)\Bigg]
\end{aligned} \tag{C.3}$$

while all other integrals which appear in (60) cancel each other (which will be shown in an example later). It can be verified easily that

$$\begin{aligned} \lim_{p_f \to 0} \Delta_1 &= \delta, &\text{(C.4)} \\ \lim_{p_f \to 0} \Delta_2 &= 0 \;\text{ with } \Delta_2 \sim |\mathbf{p}_f| &\text{(C.5)} \end{aligned}$$

according to definitions (49), (50) and (77). With these limits the behavior of ι_1 for small p_f can be calculated in a straight forward way:

$$\lim_{p_f \to 0} \iota_1 = \frac{16\pi A E_f^2 p_i^2 \sin^2\Theta_i}{(E_i - cp_i\cos\Theta_i)^2\delta^2}. \tag{C.6}$$

For (C.2) and (C.3), however, there is more effort to be invested. As it is $\sqrt{\Delta_2^2 + 4p_i^2p_f^2\sin^2\Theta_i} \to 0$ and $\ln\Bigg(\Big(\Delta_2^2 + 4p_i^2p_f^2\sin^2\Theta_i - \sqrt{\Delta_2^2 + 4p_i^2p_f^2\sin^2\Theta_i} \times (\Delta_1 + \Delta_2) + \Delta_1\Delta_2\Big)/\Big(-\Delta_2^2 - 4p_i^2p_f^2\sin^2\Theta_i - \sqrt{\Delta_2^2 + 4p_i^2p_f^2\sin^2\Theta_i}(\Delta_1 - \Delta_2) + \Delta_1\Delta_2\Big)\Bigg) \to 0$ for $p_f \to 0$, one has to use the rule of L'Hospital. If one rewrites

$$\Delta_2 = \Psi p_f \tag{C.7}$$

with

$$\Psi := -2\frac{\hbar}{c}\omega + 2p_i\cos\Theta_i \tag{C.8}$$

this rule leads to

$$\begin{aligned} &\lim_{p_f \to 0}\Bigg[\frac{1}{\sqrt{\Delta_2^2 + 4p_i^2p_f^2\sin^2\Theta_i}} \times \\ &\times \;\; \ln\left(\frac{\Delta_2^2 + 4p_i^2p_f^2\sin^2\Theta_i - \sqrt{\Delta_2^2 + 4p_i^2p_f^2\sin^2\Theta_i}(\Delta_1 + \Delta_2) + \Delta_1\Delta_2}{-\Delta_2^2 - 4p_i^2p_f^2\sin^2\Theta_i - \sqrt{\Delta_2^2 + 4p_i^2p_f^2\sin^2\Theta_i}(\Delta_1 - \Delta_2) + \Delta_1\Delta_2}\right)\Bigg] \\ &= \;\; -\frac{2}{\delta}; \end{aligned} \tag{C.9}$$

thus

$$\lim_{p_f \to 0} \iota_2 = \frac{4\pi A p_i^2 c^2 \sin^2 \Theta_i}{(E_i - c p_i \cos \Theta_i)^2 \delta}. \tag{C.10}$$

The limit of (C.3) can also be calculated by using (C.7). It is

$$\begin{aligned}
\iota_3 &= -\frac{4\pi\hbar^2\omega^2 p_i^2 \sin^2 \Theta_i A}{E_i - c p_i \cos \Theta_i} \Bigg[-\frac{p_f^2 (2\Delta_1 \Psi c + 2\Psi^2 E_f + 8 p_i^2 \sin^2 \Theta_i E_f)}{p_f^2(-\Delta_2^2 + \Delta_1^2 - 4p_i^2 \sin^2 \Theta_i)((\Psi E_f + \Delta_1 c)^2 + 4m^2 c^4 p_i^2 \sin^2 \Theta_i)} \\
&\times \frac{p_f^2 c (\Psi E_f + \Delta_1 c)}{p_f^2((\Psi E_f + \Delta_1 c)^2 + 4m^2 c^4 p_i^2 \sin^2 \Theta_i)} \\
&\times \frac{1}{p_f \sqrt{(\Psi E_f + \Delta_1 c)^2 + 4m^2 c^4 p_i^2 \sin^2 \Theta_i)}} \\
&\times \ln \Bigg(\Big((E_f + p_f c)(4 p_i^2 p_f^2 \sin^2 \Theta_i (E_f - p_f c) + (\Delta_1 + \Psi p_f)(p_f(\Psi E_f + \Delta_1 c) \\
&- p_f \sqrt{(\Psi E_f + \Delta_1 c)^2 + 4m^2 c^4 p_i^2 \sin^2 \Theta_i)})) \Big) \Big((E_f - p_f c)(4 p_i^2 p_f^2 \sin^2 \Theta_i (-E_f - p_f c) \\
&+ (\Delta_1 - \Psi p_f)(p_f(\Psi E_f + \Delta_1 c) - p_f \sqrt{(\Psi E_f + \Delta_1 c)^2 + 4m^2 c^4 p_i^2 \sin^2 \Theta_i)})) \Big)^{-1} \Bigg) \Bigg]
\end{aligned} \tag{C.11}$$

While p_f can simply be reduced in the fractions, one has to use the rule of L'Hospital again for the logarithmic part because it is $p_f \sqrt{(\Psi E_f + \Delta_1 c)^2 + 4m^2 c^4 p_i^2 \sin^2 \Theta_i} \to 0$ and the logarithm $\to 0$ for $p_f \to 0$. Its limit is

$$\begin{aligned}
&\lim_{p_f \to 0} \frac{1}{p_f \sqrt{(\Psi E_f + \Delta_1 c)^2 + 4m^2 c^4 p_i^2 \sin^2 \Theta_i}} \\
&\times \ln \Bigg(\Big((E_f + p_f c)(4 p_i^2 p_f^2 \sin^2 \Theta_i (E_f - p_f c) + (\Delta_1 + \Psi p_f)(p_f(\Psi E_f + \Delta_1 c) \\
&- p_f \sqrt{(\Psi E_f + \Delta_1 c)^2 + 4m^2 c^4 p_i^2 \sin^2 \Theta_i)})) \Big) \Big((E_f - p_f c)(4 p_i^2 p_f^2 \sin^2 \Theta_i (-E_f - p_f c) \\
&+ (\Delta_1 - \Psi p_f)(p_f(\Psi E_f + \Delta_1 c) - p_f \sqrt{(\Psi E_f + \Delta_1 c)^2 + 4m^2 c^4 p_i^2 \sin^2 \Theta_i)})) \Big)^{-1} \Bigg) \Bigg] \\
&= -\frac{2}{E_f \Delta_1} \bigg|_{p_f \to 0} = -\frac{2}{E_f \delta};
\end{aligned} \tag{C.12}$$

thus the whole limit yields after some further calculations

$$\lim_{p_f \to 0} \iota_3 = \frac{8\pi\hbar^2\omega^2 p_i^2 \sin^2 \Theta_i A}{(E_i - c p_i \cos \Theta_i)\delta^2 E_f}. \tag{C.13}$$

Finally, if one inserts (14), the sum of (C.6), (C.10) and (C.13) leads to (81).

All other terms which appear in (60) vanish. For this purpose one should regroup all terms according to their origin. As an example let's consider the three contributions which have arisen from $\int\limits_{\Theta_f=0}^{\pi} \int\limits_{\Phi=0}^{2\pi} \frac{a_2 \cos \Phi}{\alpha \cos \Phi + \beta} d\Phi d\Theta_f$. For this integral it follows

$$
\begin{aligned}
& \int\limits_{\Theta_f=0}^{\pi} \int\limits_{\Phi=0}^{2\pi} \frac{a_2 \cos\Phi}{\alpha\cos\Phi+\beta} d\Phi d\Theta_f \\
= \quad & -\frac{2\pi Ac}{(E_i - cp_i\cos\Theta_i)p_f} \ln\left(\frac{E_f+p_fc}{E_f-p_fc}\right) \\
- \quad & \frac{2\pi Ac^2}{E_i - cp_i\cos\Theta_i} \Bigg[-\frac{\Delta_2}{\sqrt{\Delta_2^2+4p_i^2p_f^2\sin^2\Theta_i}p_fc} \\
\times \quad & \ln\left(\frac{\Delta_2^2+4p_i^2p_f^2\sin^2\Theta_i-\sqrt{\Delta_2^2+4p_i^2p_f^2\sin^2\Theta_i}(\Delta_1+\Delta_2)+\Delta_1\Delta_2}{-\Delta_2^2-4p_i^2p_f^2\sin^2\Theta_i-\sqrt{\Delta_2^2+4p_i^2p_f^2\sin^2\Theta_i}(\Delta_1-\Delta_2)+\Delta_1\Delta_2}\right) \\
- \quad & \frac{\Delta_2E_f+\Delta_1p_fc}{p_fc\sqrt{(\Delta_2E_f+\Delta_1p_fc)^2+4m^2c^4p_i^2p_f^2\sin^2\Theta_i^2}} \\
\times \quad & \ln\Bigg(\bigg((E_f+p_fc)(4p_i^2p_f^2\sin^2\Theta_i(E_f-p_fc)+(\Delta_1+\Delta_2)((\Delta_2E_f+\Delta_1p_fc) \\
- \quad & \sqrt{(\Delta_2E_f+\Delta_1p_fc)^2+4m^2c^4p_i^2p_f^2\sin^2\Theta_i}))\bigg)\bigg((E_f-p_fc)(4p_i^2p_f^2\sin^2\Theta_i(-E_f-p_fc) \\
+ \quad & (\Delta_1-\Delta_2)((\Delta_2E_f+\Delta_1p_fc)-\sqrt{(\Delta_2E_f+\Delta_1p_fc)^2+4m^2c^4p_i^2p_f^2\sin^2\Theta_i}))\bigg)^{-1}\Bigg)\Bigg] \\
\xrightarrow{\hbar\omega\to E_{kin,i}} \quad & \frac{2\pi Ac}{E_i-cp_i\cos\Theta_i}\left[-\frac{2c}{E_f}+\Psi\left(-\frac{2}{\delta}\right)+\left(\Psi E_f+\delta c\right)\frac{2}{E_f\delta}\right] \\
= \quad & 0
\end{aligned}
\tag{C.14}
$$

where we have used (C.9), (C.12) and

$$\lim_{p_f\to 0}\frac{1}{p_f}\ln\left(\frac{E_f+p_fc}{E_f-p_fc}\right)=\frac{2c}{E_f} \tag{C.15}$$

in the limiting step. Of course, this term has to vanish because $a_2 \sim p_f$, but the concrete calculation after having integrated over Φ and Θ_f is much more complicated. Therefore we have just given an example here. Similarly, all other terms cancel so that only the limits of $\iota_i,\ i \in \{1,2,3\}$, stay.

Appendix D. Comparison with Geant 4

As mentioned in the introduction cross sections for Bremsstrahlung can be found in the Geant 4 database (Agostinelli et al., 2003).$\sigma(E_{kin,i})$. Geant 4 contains data for the total cross section σ, the singly differential cross section $d\sigma/d\omega$ and a singly differential cross section $d\sigma/d\Omega_i$ depending on Θ_i, but not on ω. Figure D.12 shows the comparison of the singly differential cross section $d\sigma/d\omega(E_{kin,i},\omega)$; here the singly differential cross section for Bremsstrahlung which can be obtained by integrating over Φ, Θ_i and Θ_f, reads

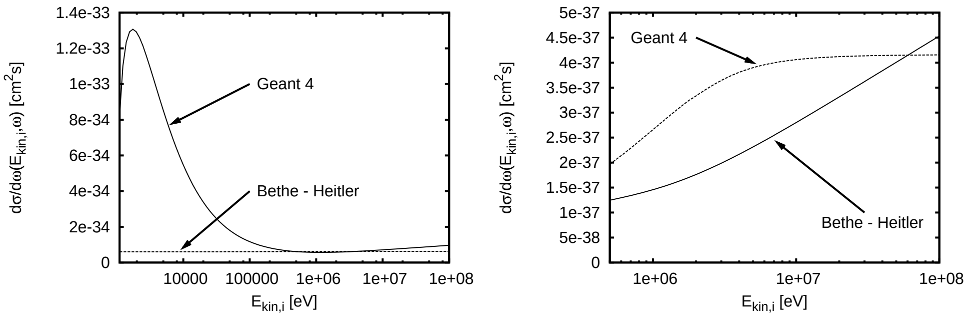

a) $\hbar\omega = 1$ keV b) $\hbar\omega = 150$ keV

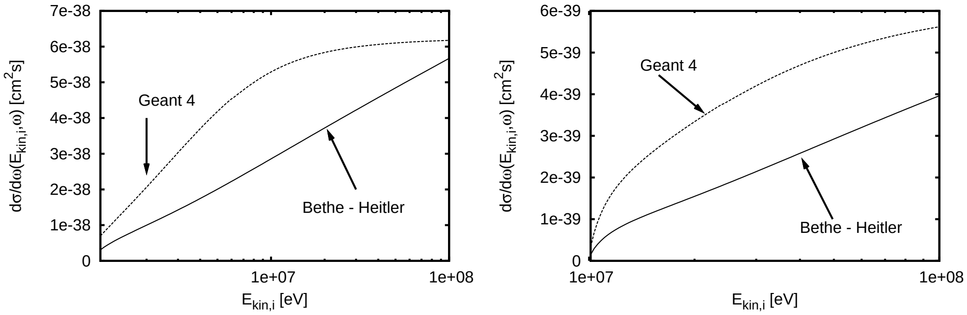

c) $\hbar\omega = 1$ MeV d) $\hbar\omega = 10$ MeV

Figure D.12: Singly differential cross section $d\sigma/d\omega$ (on linear scale) for $Z = 7$ (N_2) from the between Bethe - Heitler approximation (D.1) and the data of Geant 4 as a function of incident electron energy $E_{kin,i}$ and photon frequency ω. In the different panels, the energy of the emitted photon is fixed to $\hbar\omega = 1$ keV (a), 150 keV (b), 1 MeV (c) and 10 MeV (d).

(Bethe and Heitler, 1934; Heitler, 1944)

$$\begin{aligned}
\frac{d\sigma}{d\omega} &= \bar{\phi}\frac{1}{\omega}\frac{p_f}{p_i}\left\{\frac{4}{3} - 2E_iE_f\frac{c^2p_f^2+c^2p_i^2}{c^4p_f^2p_i^2} + m_e^2c^4\left(\frac{\tilde{\epsilon}E_f}{c^3p_i^3}+\frac{\epsilon E_i}{c^3p_f^3}-\frac{\epsilon\tilde{\epsilon}}{c^2p_ip_f}\right)\right. \\
&+ L\left[\frac{8}{3}\frac{E_iE_f}{c^2p_ip_f}+\frac{\hbar^2\omega^2}{c^6p_i^3p_f^3}\left(E_i^2E_f^2+c^4p_i^2p_f^2\right)\right. \\
&+ \left.\left.\frac{m_e^2c^4\hbar\omega}{2c^2p_ip_f}\left(\frac{E_iE_f+c^2p_i^2}{c^3p_i^3}\tilde{\epsilon}-\frac{E_iE_f+c^2p_f^2}{c^3p_f^3}\epsilon+\frac{2\hbar\omega E_iE_f}{c^4p_i^2p_f^2}\right)\right]\right\} \qquad \text{(D.1)}
\end{aligned}$$

with

$$\begin{aligned}
L &= 2\log\frac{E_iE_f+p_ip_fc^2-m_e^2c^4}{m_ec^2\hbar\omega}, && \text{(D.2)} \\
\tilde{\epsilon} &= 2\log\frac{E_i+p_ic}{m_ec^2}, && \text{(D.3)} \\
\epsilon &= 2\log\frac{E_f+p_fc}{m_ec^2}, && \text{(D.4)} \\
\bar{\phi} &= \frac{Z^2r_0^2}{137} && \text{(D.5)}
\end{aligned}$$

where $r_0 \approx 2.80 \cdot 10^{-13}$cm is the classical electron radius.

The Geant 4 database uses theoretical formula for both the low and high energy range which also includes the shielding due to the outer electrons which is actually not included in (1). (D.1) and (Agostinelli et al., 2003) vary from each other for all related electron and photon energies. Figure D.12 shows a qualitatvely different behaviour as for the based data (Seltzer and Berger, 1985) mainly contains data for high atomic numbers which are not appropriate to describe Bremsstrahlung in air. Schaffer et al. (1996), however, argue that the theory of Bethe and Heitler is good for an energy range of 1 keV - 1 GeV as long as $Z < 29$, hence appropriate for the molecules of air.

Appendix E. Comparison with Lehtinen (2000)

Figure E.13 shows the comparison of (60) and the doubly differential cross section used by Lehtinen. In all plots the photon energy $\hbar\omega$ amounts 50% of the incident electron energy. Qualitatively there is a good agreement, but

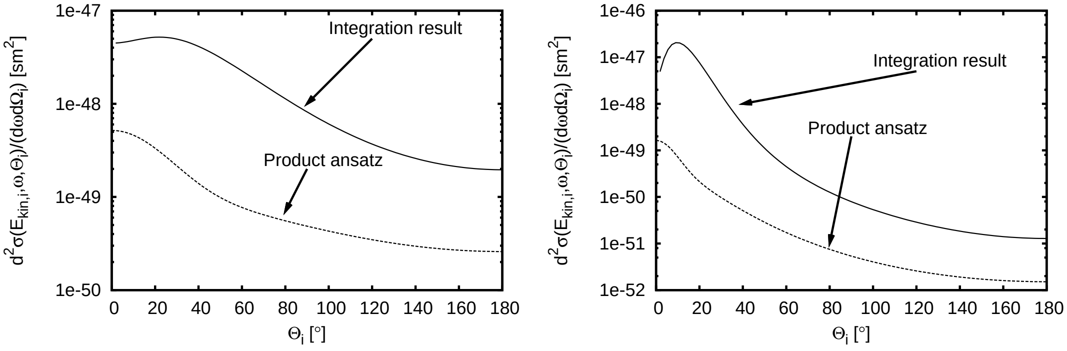

a) $E_{kin,i} = 150$ keV   b) $E_{kin,i} = 1$ MeV

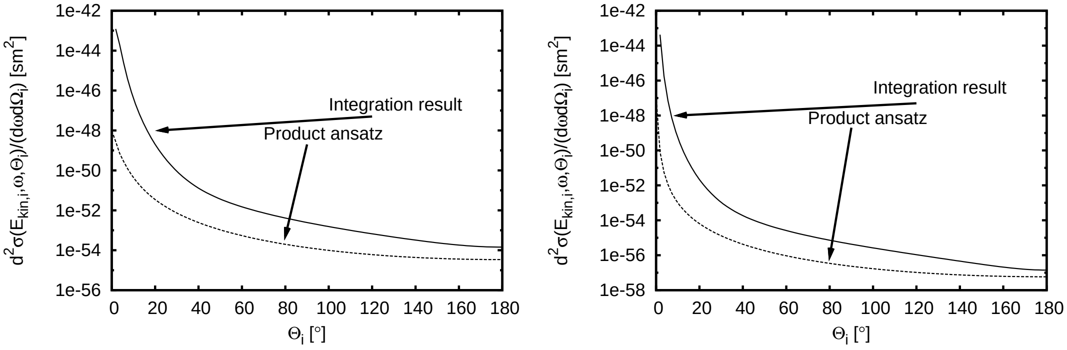

c) $E_{kin,i} = 10$ MeV   d) $E_{kin,i} = 100$ MeV

Figure E.13: Comparison of the product ansatz from Lehtinen (2000) with our result (60) of the integration of (1) for different electron energies ($Z = 7$): doubly differential cross section versus the scattering angle Θ_i between incident electron and emitted photon. The ratio between the photon energy $\hbar\omega$ and the kinetic electron energy $E_{kin,i}$ is fixed to 50%.

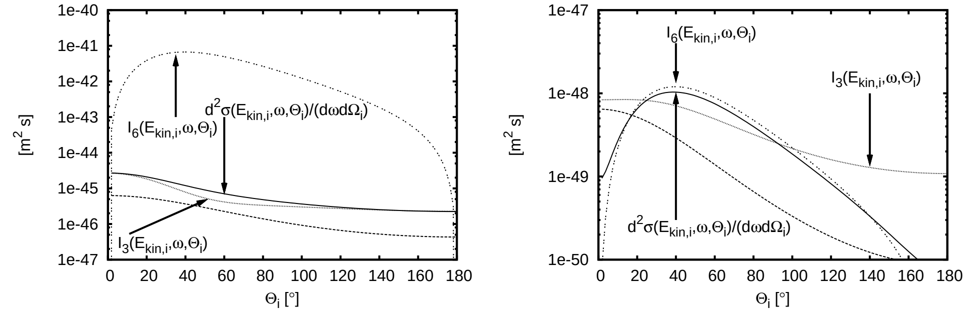

a) $E_{kin,i} = 100$ keV, $\hbar\omega = 1$ keV b) $E_{kin,i} = 100$ keV, $\hbar\omega = 95$ keV

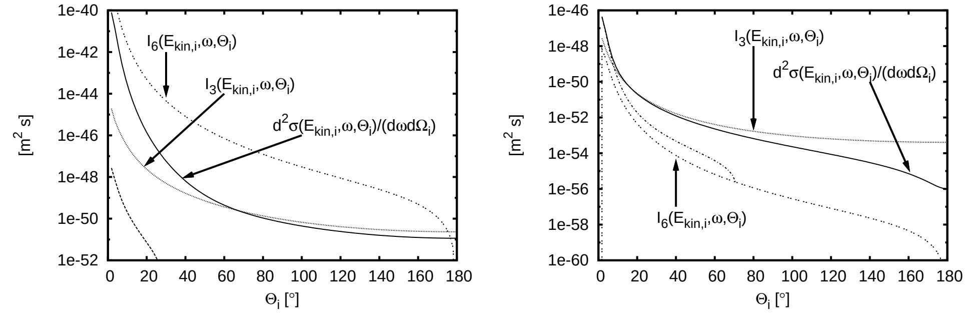

c) $E_{kin,i} = 10$ MeV, $\hbar\omega = 100$ keV d) $E_{kin,i} = 10$ MeV, $\hbar\omega = 9.5$ MeV

Figure F.14: Contribution of (61) - (66) to (60) in a semilog plot for different electron and photon energies ($Z = 7$).

both curves deviate some orders of magnitude. According to (Jackson, 1975) Lehtinen uses a product ansatz for the angular and the frequency part; here the angular part is a non-quantum mechanical expression (Jackson, 1975). The product ansatz is said to be valid for very high electron energies and very small photon energies; therefore this cross section does not cover the whole energy range needed to simulate Bremsstrahlung in air.

Appendix F. Contribution of the integrals

As equation (60) is rather complicated, it is interesting to see which terms have the most important contribution. Figure F.14 shows the contribution of all parts to the final result in a logarithmic scale while Fig. F.15 shows the same in a linear scale. In all cases, i.e. low and high electron energies and low and high ratios between $\hbar\omega$ and $E_{kin,i}$, the main contribution comes

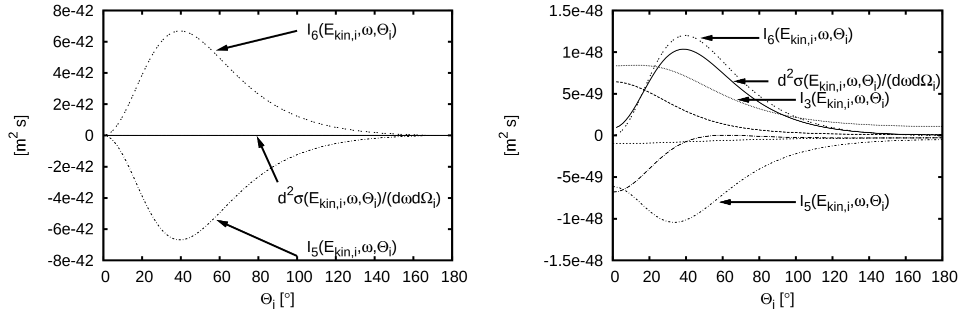

a) $E_{kin,i} = 100$ keV, $\hbar\omega = 1$ keV b) $E_{kin,i} = 100$ keV, $\hbar\omega = 95$ keV

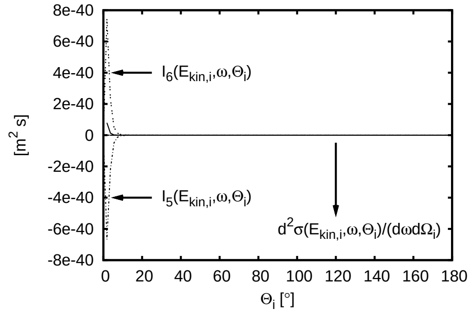

c) $E_{kin,i} = 10$ MeV, $\hbar\omega = 100$ keV

Figure F.15: Contribution of (61) - (66) to (60) in a linear plot for different electron and photon energies ($Z = 7$).

from (63). It is important to state that not all contributions can be seen in figure F.14 because some of the terms have negative values which, however, are shown in figure F.15. So one might think that for $E_{kin,i} = 100$ keV and $\hbar\omega = 1$ keV, equation (66) has the largest contribution, but as figure F.15 shows, (65) has nearly the same absolute value, but opposite sign; therefore they cancel. Thus the third integral (63) is the most important one. The same holds for other electron energies and ratios between $\hbar\omega$ and $E_{kin,i}$. We conclude that (63) is the dominant contribution for all relevant parameter values.

Appendix G. Conservation of energy and momentum

One can also gain information on the scattering angle Θ_i for high electron energies from the conservation of energy and momentum,

$$\begin{aligned} E_i + E_q &= E_f + \hbar\omega, & \text{(G.1)} \\ \mathbf{p}_i + \mathbf{q} &= \mathbf{p}_f + \hbar\mathbf{k} & \text{(G.2)} \end{aligned}$$

where $E_{i,f}$ and $p_{i,f}$ are the energy and the momentum of the electron in the initial and final state. $\hbar\mathbf{k}$ is the momentum of the photon which is related to its energy $\hbar\omega$ through

$$\hbar|\mathbf{k}| = \frac{\hbar}{c}\omega, \tag{G.3}$$

and E_q and $\mathbf{q}$ are the energy and the momentum of the virtual photon between electron and nucleus. $\mathbf{q}$ changes the momentum of the nucleus. But the contribution to the kinetic energy can be neglected; thus $E_q \equiv 0$ and

$$\begin{aligned} E_i &= E_f + \hbar\omega, & \text{(G.4)} \\ \mathbf{p}_i - \hbar\mathbf{k} &= \mathbf{p}_f - \mathbf{q}. & \text{(G.5)} \end{aligned}$$

Squaring (G.5) and using $\mathbf{p}_i \cdot \mathbf{k} = |\mathbf{p}_i||\mathbf{k}| \cos\sphericalangle(\mathbf{p}_i, \mathbf{k}) = p_i\ k \cos\Theta_i$, the angle Θ_i is:

$$\cos\Theta_i = \frac{(\mathbf{p}_f - \mathbf{q})^2 - p_i^2 - \hbar^2 k^2}{-2\hbar p_i k}. \tag{G.6}$$

By using (G.4) and the relativistic energy-momentum relation (2) we get an expression for the momentum of the electron in the final state

$$p_f = \sqrt{p_i^2 + \hbar^2 k^2 - 2\hbar k \sqrt{p_i^2 + m_e^2 c^2}} \tag{G.7}$$

which leads to

$$\cos\Theta_i = \frac{2\hbar\omega\frac{E_i}{c} + 2q\sqrt{(E_i - \hbar\omega)^2 - m_e^2 c^4}\cos\sphericalangle(\mathbf{p}_f, \mathbf{q}) - cq^2}{2\hbar\omega p_i}. \tag{G.8}$$

Although this is an analytical expression for the scattering angle Θ_i one should take into account that it depends on the vector $\mathbf{q}$ of the virtual photon which is not known in forehand. Thus, depending on $\mathbf{q}$, only a statistical statement can be made about Θ_i.

It is, however, possible to investigate the limit of (G.8) for high electron energies which yields

$$\lim_{E_i \to \infty} \cos\Theta_i = 1 + \frac{cq}{\hbar\omega}\cos\sphericalangle(\mathbf{p}_f, \mathbf{q}) \tag{G.9}$$

As $\Theta_i \in \mathbb{R} \Leftrightarrow \cos\Theta_i \in [-1, +1]$ and $c, q, \hbar\omega > 0$ we can conclude that

$$\cos\sphericalangle(\mathbf{p}_f, \mathbf{q}) \leq 0 \tag{G.10}$$

Especially for $|\frac{cq}{\hbar\omega}\cos\sphericalangle(\mathbf{p}_f, \mathbf{q})| \ll 1, \Theta_i \approx 0$, i.e., the photon is mainly emitted in forward direction.

If, additionally, the photon energy $\hbar\omega$ also increases more and more (for high electron energies) it is

$$\lim_{\hbar\omega \to \infty}\Big(1 + \frac{cq}{\hbar\omega}\cos\sphericalangle(\mathbf{p}_f, \mathbf{q})\Big) = 1; \tag{G.11}$$

thus

$$\lim_{E_i, \hbar\omega \to \infty} \Theta_i = 0. \tag{G.12}$$

Hence, we conclude from simple considerations about energy and momentum conservation that the photon is mainly scattered in forward direction if the energies of electron and photon are both very high.

Appendix H. Approximation for Θ_i

In order to obtain (108) we calculate the derivative of (81) after Θ_i:

$$\begin{aligned}
\frac{\partial}{\partial\Theta_i}\left(\frac{d^2\sigma}{d\omega\sin\Theta_i d\Theta_i}\right) &= \frac{Z^2\alpha_{fine}^3 h^2}{\pi}\frac{|\mathbf{p}_f||\mathbf{p}_i|}{\omega}\left[\frac{4\frac{\hbar}{c}\omega|\mathbf{p}_i|\sin\Theta_i}{\delta^3(\Theta_i)}\times\right. \\
\times &\quad \left(\frac{\sin^2\Theta_i}{(E_i-c|\mathbf{p}_i|\cos\Theta_i)^2}(4E_f^2+\delta(\Theta_i)c^2)+\frac{2\hbar^2\omega^2}{E_f}\frac{\sin^2\Theta_i}{E_i-c|\mathbf{p}_i|\cos\Theta_i}\right) \\
+ &\quad \frac{1}{\delta^2(\Theta_i)}\left(\frac{2\sin\Theta_i\cos\Theta_i(E_i-c|\mathbf{p}_i|\cos\Theta_i)-2c|\mathbf{p}_i|\sin^3\Theta_i}{(E_i-c|\mathbf{p}_i|\cos\Theta_i)^3}\right. \\
\times &\quad (4E_f^2+\delta(\Theta_i)c^2)-\frac{2\hbar c\omega|\mathbf{p}_i|\sin^3\Theta_i}{(E_i-c|\mathbf{p}_i|\cos\Theta_i)^2} \\
+ &\quad \left.\left.\frac{2\hbar^2\omega^2}{E_f}\frac{2\sin\Theta_i\cos\Theta_i(E_i-c|\mathbf{p}_i|\cos\Theta_i)-c|\mathbf{p}_i|\sin^3\Theta_i}{(E_i-c|\mathbf{p}_i|\cos\Theta_i)^2}\right)\right]
\end{aligned} \tag{H.1}$$

with definition (77) for δ. In order to calculate the extrema one has to set equation (H.1) equal to zero:

$$\begin{aligned}
0 &= 4\frac{\hbar}{c}\omega|\mathbf{p}_i|\left[\frac{\sin^2\Theta_i}{(E_i-c|\mathbf{p}_i|\cos\Theta_i)^2}(4E_f^2+\delta(\Theta_i)c^2)\right. \\
&+ \left.\frac{2\hbar^2\omega^2}{E_f}\frac{\sin^2\Theta_i}{E_i-c|\mathbf{p}_i|\cos\Theta_i}\right](E_i-c|\mathbf{p}_i|\cos\Theta_i)^3 \\
&+ \delta(\Theta_i)\left[2(E_i\cos\Theta_i-c|\mathbf{p}_i|)(4E_f^2+\delta(\Theta_i)c^2)\right. \\
&- 2\hbar c\omega|\mathbf{p}_i|\sin^2\Theta_i(E_i-c|\mathbf{p}_i|\cos\Theta_i) \\
&+ \frac{2\hbar^2\omega^2}{E_f}\left(2\cos\Theta_i(E_i-c|\mathbf{p}_i|\cos\Theta_i)^2\right. \\
&- \left.\left.c|\mathbf{p}_i|\sin^2\Theta_i(E_i-c|\mathbf{p}_i|\cos\Theta_i)\right)\right].
\end{aligned} \tag{H.2}$$

As $\delta(\Theta_i)\sim\cos\Theta_i$, expression (H.2) is quartic in $\cos\Theta_i$; therefore (H.2) can be solved analytically in principle, but the solution will be long and complicated. Figure 2 also shows that the angles for maximal scattering are very small for relativistic electrons, therefore one can approximate $\cos\Theta_i\approx 1$ and $\sin\Theta_i\approx\Theta_i$. This leads to

$$\delta(\Theta_i)\approx-|\mathbf{p}_i|^2-\left(\frac{\hbar}{c}\omega\right)^2+2\frac{\hbar}{c}\omega|\mathbf{p}_i|=\delta(\Theta_i=0)=:\delta_0 \tag{H.3}$$

and

$$
\begin{aligned}
0 &= 4\frac{\hbar}{c}\omega|\mathbf{p}_i|\left[\Theta_i^2(4E_f^2+\delta_0 c^2)+\frac{2\hbar^2\omega^2}{E_f}\Theta_i^2(E_i-c|\mathbf{p}_i|)\right] \\
&+ \delta_0\left[2(4E_f^2+\delta_0 c^2)-2\hbar c\omega|\mathbf{p}_i|\Theta_i^2+\frac{2\hbar^2\omega^2}{E_f}\left(2(E_i-c|\mathbf{p}_i|)-c|\mathbf{p}_i|\Theta_i^2\right)\right]
\end{aligned}
\tag{H.4}
$$

with solution

$$
\Theta_i=\sqrt{\frac{-\frac{\delta_0}{\hbar\omega}(4E_f^2+\delta_0c^2)-\frac{2\delta_0\hbar\omega}{E_f}(E_i-c|\mathbf{p}_i|)}{2\frac{|\mathbf{p}_i|}{c}\left[4E_f^2+\delta_0c^2+\frac{2\hbar^2\omega^2}{E_f}(E_i-c|\mathbf{p}_i|)\right]-|\mathbf{p}_i|\delta_0c-\frac{\hbar\omega}{E_f}c|\mathbf{p}_i|\delta_0}}
\tag{H.5}
$$

Appendix I. C++ code

In this section we present a C++ code which can be used to create data tables for the doubly differential cross sections (60) and (94). The code consists of three parts: In the beginning there is a header which defines all used physical constants and the functions for Bremsstrahlung and pair production. These lines have to appear in the beginning of a C++ code. Then the functions for Bremsstrahlung and pair production follow which can be placed any where else in the code.

The function to calculate the doubly differential cross section for Bremsstrahlung can be called as

```
brems   (E_kin,omega,Theta_i)
```

where E_kin denotes the kinetic energy of the incident electron in Joule, omega is the frequency of the emitted photon in s^{-1} and Theta_i is the scattering angle. The function to calculate the doubly differential cross section for pair production can be called as

```
pair_pr(E_kin,omega,Theta_p)
```

where E_kin denotes the kinetic energy of the created positron in Joule, omega the frequency of the incident photon in s^{-1} and Theta_p the angle between both.

The whole code to calculate the doubly differential cross sections for Bremsstrahlung and pair production reads

```
// Doubly differential cross section for
// Bremsstrahlung and pair production
// ------------------------------------------
// (C) Christoph Koehn, Ute Ebert
// Centrum Wiskunde en Informatica
// P.O. Box 94079, NL-1090 GB, Amsterdam

#include <math.h>

// Define physical constants
// to be set in the beginning of the code
#define hbar (1.054571726*pow(10,-34))
           // Planck's constant
#define SpeedOfLight 299792458.0
           // Speed of light in vacuum
#define SpeedOfLight2 pow(299792458,2)
           // Speed of light in vacuum, squared
#define electronMass (9.10938291*pow(10,-31))
           // Mass of an electron
#define electronCharge (1.602176565*pow(10,-19))
           // Charge of an electron (without sign)
#define rest_energy (electronMass*SpeedOfLight2)
          // Rest energy of the electron
#define alpha_fine (7.2973525698*pow(10,-3))
              // fine structure constant
#define PI 3.14159265358979
           // PI



// Define functions for doubly differential
// cross section for Bremstrahlung and
// pair production, also to be set in the
// beginning of the code


// Doubly differential cross section for Bremsstrahlung
// which depends on the kinetic energy of the incident
   electron,
// frequency of the emitted photon and angle between
   both
// (in radian)
double brems(double E_kin,double omega,double Theta_i);

// Doubly differential cross section for pair
   production
// which depends on the kinetic energy of the generated
    positron,
// frequency of the incident photon and angle between
   both
// (in radian)
double pair_pr(double E_kin,double omega,double Theta_p
   );


//―――――――――――――――――――――――――――――――――――――――――――――――――――――――――――――――――――――


// functions for calculating doubly differential
// cross sections for Bremsstrahlung and pair
// production

// Bremsstrahlung
double brems(double E_kin,double omega,double Theta_i)
{
  int i;

  // define physical quantities: energies and momenta
  double E_i=E_kin+rest_energy; // total energy of
     incident electron
  double E_f=E_i-hbar*omega;     // total energy of
     outgoing electron
  double p_i=sqrt(pow(E_i,2)*pow(SpeedOfLight,-2)-pow(
     electronMass,2)*SpeedOfLight2);     // momentum of
     incident electron
```

```
double p_f=sqrt(pow(E_f,2)*pow(SpeedOfLight,-2)-pow(electronMass,2)*SpeedOfLight2);      // momentum of outgoing electron

// define help functions
int Z=7;       // atomic number, can be changed arbitrarily
double A=pow(Z,2)*pow(alpha_fine,3)/(4*pow(PI,2))*p_f/p_i*pow(hbar*2*PI,2)/omega;        // overall prefactor, defined in (22)
double B=pow(Z,2)*pow(alpha_fine,3)/(2*PI)*p_f/p_i*pow(hbar*2*PI,2)/omega;               // overall prefactor for Theta_i=0
// delta functions defined in (51) and (52)
double tri_1=-pow(p_i,2)-pow(p_f,2)-pow(hbar*pow(SpeedOfLight,-1)*omega,2)+2*hbar*pow(SpeedOfLight,-1)*omega*p_i*cos(Theta_i);
double tri_2=-2*hbar*pow(SpeedOfLight,-1)*omega*p_f+2*p_i*p_f*cos(Theta_i);

double I[8]={0};       // parts of the cross section
double cross=0;        // total result of cross section

// all terms which are needed for the cross section
if (Theta_i!=0)        // calculate cross section for all angles, except for 0 degree
{
  I[0]=2*PI*A/sqrt(pow(tri_2,2)+pow(2*p_i*p_f*sin(Theta_i),2))*log((pow(tri_2,2)+pow(2*p_i*p_f*sin(Theta_i),2)-(tri_1+tri_2)*sqrt(pow(tri_2,2)+pow(2*p_i*p_f*sin(Theta_i),2))+tri_1*tri_2)/(-pow(tri_2,2)-pow(2*p_i*p_f*sin(Theta_i),2)-(tri_1-tri_2)*sqrt(pow(tri_2,2)+pow(2*p_i*p_f*sin(Theta_i),2))+tri_1*tri_2))*(1+SpeedOfLight*tri_2/(p_f*(E_i-p_i*SpeedOfLight*cos(Theta_i)))-pow(p_i*SpeedOfLight*sin(Theta_i)/(E_i-SpeedOfLight*p_i*cos(Theta_i)),2)-2*pow(hbar*omega,2)*p_f*
    tri_2/(SpeedOfLight*(E_i-SpeedOfLight*p_i*cos(
    Theta_i))*(pow(tri_2,2)+pow(2*p_i*p_f*sin(
    Theta_i),2))));
I[1]=-2*PI*A*SpeedOfLight/(p_f*(E_i-SpeedOfLight*
    p_i*cos(Theta_i)))*log((E_f+SpeedOfLight*p_f)/(
    E_f-SpeedOfLight*p_f));
I[2]=2*PI*A/sqrt(pow(tri_2*E_f+tri_1*p_f*
    SpeedOfLight,2)+pow(2*rest_energy*p_i*p_f*sin(
    Theta_i),2))*log(((E_f+p_f*SpeedOfLight)*(pow(2*
    p_i*p_f*sin(Theta_i),2)*(E_f-p_f*SpeedOfLight)+(
    tri_1+tri_2)*((tri_2*E_f+tri_1*p_f*SpeedOfLight)
    -sqrt(pow(tri_2*E_f+tri_1*p_f*SpeedOfLight,2)+
    pow(2*rest_energy*p_i*p_f*sin(Theta_i),2)))))/((
    E_f-p_f*SpeedOfLight)*(pow(2*p_i*p_f*sin(Theta_i
    ),2)*(-E_f-p_f*SpeedOfLight)+(tri_1-tri_2)*((
    tri_2*E_f+tri_1*p_f*SpeedOfLight)-sqrt(pow(tri_2
    *E_f+tri_1*p_f*SpeedOfLight,2)+pow(2*rest_energy
    *p_i*p_f*sin(Theta_i),2))))))*(-((pow(tri_2,2)+
    pow(2*p_i*p_f*sin(Theta_i),2))*(pow(E_f,3)+E_f*
    pow(p_f*SpeedOfLight,2))+p_f*SpeedOfLight*(2*(
    pow(tri_1,2)-pow(2*p_i*p_f*sin(Theta_i),2))*E_f*
    p_f*SpeedOfLight+tri_1*tri_2*(3*pow(E_f,2)+pow(
    p_f*SpeedOfLight,2))))/(pow(tri_2*E_f+tri_1*p_f*
    SpeedOfLight,2)+pow(2*rest_energy*p_i*p_f*sin(
    Theta_i),2)) -SpeedOfLight*(tri_2*E_f+tri_1*p_f*
    SpeedOfLight)/(p_f*(E_i-SpeedOfLight*p_i*cos(
    Theta_i))) -(pow(2*E_i*p_f,2)*(2*pow(tri_2*E_f+
    tri_1*p_f*SpeedOfLight,2)-pow(2*electronMass*
    SpeedOfLight2*p_i*p_f*sin(Theta_i),2))*(tri_1*
    E_f+tri_2*p_f*SpeedOfLight))/(pow(pow(tri_2*E_f+
    tri_1*p_f*SpeedOfLight,2)+pow(2*rest_energy*p_i*
    p_f*sin(Theta_i),2),2))+(8*pow(p_i*p_f*
    rest_energy*sin(Theta_i),2)*(pow(E_i,2)+pow(E_f
    ,2))-2*pow(hbar*omega*p_i*sin(Theta_i),2)*p_f*
    SpeedOfLight*(tri_2*E_f+tri_1*p_f*SpeedOfLight)
    +2*pow(hbar*omega,2)*p_f*pow(electronMass,2)*pow
    (SpeedOfLight,3)*(tri_2*E_f+tri_1*p_f*
    SpeedOfLight))/((E_i-SpeedOfLight*p_i*cos(
        Theta_i))*(pow(tri_2*E_f+tri_1*p_f*SpeedOfLight
        ,2)+pow(2*rest_energy*p_i*p_f*sin(Theta_i),2))))
        ;
    I[3]=-4*PI*A*p_f*SpeedOfLight*(tri_2*E_f+tri_1*p_f*
        SpeedOfLight)/(pow(tri_2*E_f+tri_1*p_f*
        SpeedOfLight,2)+4*pow(rest_energy*p_i*p_f*sin(
        Theta_i),2))-16*PI*pow(E_i,2)*pow(p_f,2)*A*pow(
        tri_2*E_f+tri_1*p_f*SpeedOfLight,2)/pow(pow(
        tri_2*E_f+tri_1*p_f*SpeedOfLight,2)+4*pow(
        rest_energy*p_i*p_f*sin(Theta_i),2),2);
    I[4]=4*PI*A/((-pow(tri_2,2)+pow(tri_1,2)-pow(2*p_i*
        p_f*sin(Theta_i),2))*(pow(tri_2*E_f+tri_1*p_f*
        SpeedOfLight,2)+pow(2*rest_energy*p_i*p_f*sin(
        Theta_i),2)))*(pow(hbar*omega*p_f,2)/(E_i-
        SpeedOfLight*p_i*cos(Theta_i))*(E_f*(2*pow(tri_2
        ,2)*(pow(tri_2,2)-pow(tri_1,2))+8*pow(p_i*p_f*
        sin(Theta_i),2)*(pow(tri_2,2)+pow(tri_1,2)))+p_f
        *SpeedOfLight*(2*tri_1*tri_2*(pow(tri_2,2)-pow(
        tri_1,2))-tri_1*tri_2*pow(4*p_i*p_f*sin(Theta_i)
        ,2)))/(pow(tri_2,2)+pow(2*p_i*p_f*sin(Theta_i)
        ,2))+2*pow(hbar*omega*p_i*sin(Theta_i),2)*(2*
        tri_1*tri_2*p_f*SpeedOfLight+2*pow(tri_2,2)*E_f
        +8*pow(p_i*p_f*sin(Theta_i),2)*E_f)/(E_i-p_i*
        SpeedOfLight*cos(Theta_i))+2*pow(E_i*p_f,2)*(2*(
        pow(tri_2,2)-pow(tri_1,2))*pow(tri_2*E_f+tri_1*
        p_f*SpeedOfLight,2)+8*pow(p_i*p_f*sin(Theta_i)
        ,2)*((pow(tri_1,2)+pow(tri_2,2))*(pow(E_f,2)+pow
        (p_f*SpeedOfLight,2))+4*tri_1*tri_2*E_f*p_f*
        SpeedOfLight))/(pow(tri_2*E_f+tri_1*p_f*
        SpeedOfLight,2)+pow(2*rest_energy*p_i*p_f*sin(
        Theta_i),2))+8*pow(p_i*p_f*sin(Theta_i),2)*(pow(
        E_i,2)+pow(E_f,2))*(tri_2*p_f*SpeedOfLight+tri_1
        *E_f)/(E_i-SpeedOfLight*p_i*cos(Theta_i)));
    I[5]=16*PI*pow(E_f,2)*pow(p_i,2)*pow(sin(Theta_i)
        ,2)*A/(pow(E_i-SpeedOfLight*p_i*cos(Theta_i),2)
        *(-pow(tri_2,2)+pow(tri_1,2)-4*pow(p_i,2)*pow(
        p_f,2)*pow(sin(Theta_i),2)));
}
```

```
else            // calculate cross section for 0 degree
{
  I[0]=-2*B*p_f*SpeedOfLight/(tri_2*E_f+tri_1*p_f*
     SpeedOfLight);
  I[1]=B*pow(p_f*SpeedOfLight,2)*(-pow(tri_1,2)+pow(
     tri_2,2))/(tri_2*pow(tri_2*E_f+tri_1*p_f*
     SpeedOfLight,2))*log((tri_1+tri_2)/(tri_1-tri_2)
     );
  I[2]=B*(2*tri_1*E_f*p_f*SpeedOfLight+tri_2*(pow(E_f
     ,2)+pow(p_f*SpeedOfLight,2)))/(pow(tri_2*E_f+
     tri_1*p_f*SpeedOfLight,2))*log((E_f+p_f*
     SpeedOfLight)/(E_f-p_f*SpeedOfLight));
  I[3]=-B*pow((4*E_i*p_f)/(tri_2*E_f+tri_1*p_f*
     SpeedOfLight),2);
  I[4]=-8*B*pow(E_i*p_f,2)*(tri_1*E_f+tri_2*p_f*
     SpeedOfLight)/(pow(tri_2*E_f+tri_1*p_f*
     SpeedOfLight,3))*log(((tri_1-tri_2)*(E_f-p_f*
     SpeedOfLight))/((tri_1+tri_2)*(E_f+p_f*
     SpeedOfLight)));
  I[5]=-B*pow(2*hbar*p_f*omega,2)/((tri_2*E_f+tri_1*
     p_f*SpeedOfLight)*(E_i-p_i*SpeedOfLight)*tri_2);
  I[6]=2*B*pow(hbar*p_f*omega,2)*(2*tri_1*tri_2*E_f+
     p_f*SpeedOfLight*(pow(tri_1,2)+pow(tri_2,2)))/(
     pow(tri_2*E_f+tri_1*p_f*SpeedOfLight,2)*(E_i-p_i
     *SpeedOfLight)*pow(tri_2,2))*log((tri_1+tri_2)/(
     tri_1-tri_2));
  I[7]=2*B*pow(hbar*omega,2)*p_f*(pow(E_f,2)-pow(p_f*
     SpeedOfLight,2))/(pow(tri_2*E_f+tri_1*p_f*
     SpeedOfLight,2)*(E_i-SpeedOfLight*p_i)*
     SpeedOfLight)*log((E_f-p_f*SpeedOfLight)/(E_f+
     p_f*SpeedOfLight));
}

// sum up all terms to get value for cross section
for (i=0;i<=7;i++)
{
  cross=cross+I[i];
}
```

```
  return cross; // give back result of cross section
     calculation
}


// pair production
double pair_pr(double E_kin,double omega,double Theta_p
   )
{
  int i;

  // define physical quantities: energies and momenta
  double E_p=E_kin+rest_energy;           // total energy
      of created positron
  double E_m=(hbar*omega-rest_energy)-E_kin;       //
     total energy of created electron
  double p_p=sqrt(pow(E_p,2)*pow(SpeedOfLight,-2)-pow(
     electronMass,2)*SpeedOfLight2);     // momentum of
     created positron
  double p_m=sqrt(pow(E_m,2)*pow(SpeedOfLight,-2)-pow(
     electronMass,2)*SpeedOfLight2);       // momentum of
     created electron

  // define help functions
  int Z=7;        // atomic number, can be changed
     arbitrarily
  double A=pow(Z,2)*pow(alpha_fine,3)*SpeedOfLight2*p_p
     *p_m/(4*pow(PI,2)*(hbar*2*PI)*pow(omega,3));
     // overall prefactor, defined in (107)
  double B=pow(Z,2)*pow(alpha_fine,3)*SpeedOfLight2*p_p
     *p_m/(2*PI*(hbar*2*PI)*pow(omega,3));
     // overall prefactor for Theta_p=0 and Theta_p=180
      degree
  // delta functions defined in (108) and (109)
  double tri_1=-pow(p_p,2)-pow(p_m,2)-pow(hbar*pow(
     SpeedOfLight,-1)*omega,2)+2*hbar*pow(SpeedOfLight
     ,-1)*omega*p_p*cos(Theta_p);
```

```
double tri_2=2*hbar*pow(SpeedOfLight,-1)*omega*p_m-2*
   p_p*p_m*cos(Theta_p);

double I[8]={0};         // parts of the cross section
double cross=0;          // total result of cross
   section

// all terms which are needed for the cross section
if (Theta_p!=0 && Theta_p!=PI)          // calculate
   cross section for all angles, except for 0 and 180
    degree
{
  I[0]=2*PI*A/sqrt(pow(tri_2,2)+pow(2*p_p*p_m*sin(
     Theta_p),2))*log((pow(tri_2,2)+pow(2*p_p*p_m*sin
     (Theta_p),2)-(tri_1+tri_2)*sqrt(pow(tri_2,2)+pow
     (2*p_p*p_m*sin(Theta_p),2))+tri_1*tri_2)/(-pow(
     tri_2,2)-pow(2*p_p*p_m*sin(Theta_p),2)-(tri_1-
     tri_2)*sqrt(pow(tri_2,2)+pow(2*p_p*p_m*sin(
     Theta_p),2))+tri_1*tri_2))*(-1 -SpeedOfLight*
     tri_2/(p_m*(E_p-p_p*SpeedOfLight*cos(Theta_p)))+
     pow(p_p*SpeedOfLight*sin(Theta_p)/(E_p-
     SpeedOfLight*p_p*cos(Theta_p)),2)-2*pow(hbar*
     omega,2)*p_m*tri_2/(SpeedOfLight*(E_p-
     SpeedOfLight*p_p*cos(Theta_p))*(pow(tri_2,2)+pow
     (2*p_p*p_m*sin(Theta_p),2))));
  I[1]=2*PI*A*SpeedOfLight/(p_m*(E_p-SpeedOfLight*p_p
     *cos(Theta_p)))*log((E_m+SpeedOfLight*p_m)/(E_m-
     SpeedOfLight*p_m));
  I[2]=2*PI*A/sqrt(pow(tri_2*E_m+tri_1*p_m*
     SpeedOfLight,2)+pow(2*rest_energy*p_p*p_m*sin(
     Theta_p),2))*log(((E_m+p_m*SpeedOfLight)*(pow(2*
     p_p*p_m*sin(Theta_p),2)*(E_m-p_m*SpeedOfLight)+(
     tri_1+tri_2)*((tri_2*E_m+tri_1*p_m*SpeedOfLight)
     -sqrt(pow(tri_2*E_m+tri_1*p_m*SpeedOfLight,2)+
     pow(2*rest_energy*p_p*p_m*sin(Theta_p),2)))))/((
     E_m-p_m*SpeedOfLight)*(pow(2*p_p*p_m*sin(Theta_p
     ),2)*(-E_m-p_m*SpeedOfLight)+(tri_1-tri_2)*((
     tri_2*E_m+tri_1*p_m*SpeedOfLight)-sqrt(pow(tri_2
    *E_m+tri_1*p_m*SpeedOfLight ,2)+pow(2*rest_energy
    *p_p*p_m*sin(Theta_p),2))))))*(((pow(tri_2 ,2)+
    pow(2*p_p*p_m*sin(Theta_p),2))*(pow(E_m,3)+E_m*
    pow(p_m*SpeedOfLight ,2))+p_m*SpeedOfLight*(2*(
    pow(tri_1 ,2)-pow(2*p_p*p_m*sin(Theta_p),2))*E_m*
    p_m*SpeedOfLight+tri_1*tri_2*(3*pow(E_m,2)+pow(
    p_m*SpeedOfLight ,2))))/(pow(tri_2*E_m+tri_1*p_m*
    SpeedOfLight ,2)+pow(2*rest_energy*p_p*p_m*sin(
    Theta_p),2))+SpeedOfLight*(tri_2*E_m+tri_1*p_m*
    SpeedOfLight)/(p_m*(E_p-SpeedOfLight*p_p*cos(
    Theta_p)))+(pow(2*E_p*p_m,2)*(2*pow(tri_2*E_m+
    tri_1*p_m*SpeedOfLight ,2)-pow(2*electronMass*
    SpeedOfLight2*p_p*p_m*sin(Theta_p),2))*(tri_1*
    E_m+tri_2*p_m*SpeedOfLight))/(pow(pow(tri_2*E_m+
    tri_1*p_m*SpeedOfLight ,2)+pow(2*rest_energy*p_p*
    p_m*sin(Theta_p),2),2))+(-8*pow(p_p*p_m*
    rest_energy*sin(Theta_p),2)*(pow(E_p,2)+pow(E_m
    ,2))-2*pow(hbar*omega*p_p*sin(Theta_p),2)*p_m*
    SpeedOfLight*(tri_2*E_m+tri_1*p_m*SpeedOfLight)
    +2*pow(hbar*omega,2)*p_m*pow(electronMass ,2)*pow
    (SpeedOfLight ,3)*(tri_2*E_m+tri_1*p_m*
    SpeedOfLight))/((E_p-SpeedOfLight*p_p*cos(
    Theta_p))*(pow(tri_2*E_m+tri_1*p_m*SpeedOfLight
    ,2)+pow(2*rest_energy*p_p*p_m*sin(Theta_p),2))))
    ;
I[3]=4*PI*A*p_m*SpeedOfLight*(tri_2*E_m+tri_1*p_m*
    SpeedOfLight)/(pow(tri_2*E_m+tri_1*p_m*
    SpeedOfLight ,2)+4*pow(rest_energy*p_p*p_m*sin(
    Theta_p),2))+16*PI*pow(E_p,2)*pow(p_m,2)*A*pow(
    tri_2*E_m+tri_1*p_m*SpeedOfLight ,2)/pow(pow(
    tri_2*E_m+tri_1*p_m*SpeedOfLight ,2)+4*pow(
    rest_energy*p_p*p_m*sin(Theta_p),2),2);
I[4]=4*PI*A/((-pow(tri_2 ,2)+pow(tri_1 ,2)-pow(2*p_p*
    p_m*sin(Theta_p),2))*(pow(tri_2*E_m+tri_1*p_m*
    SpeedOfLight ,2)+pow(2*rest_energy*p_p*p_m*sin(
    Theta_p),2)))*(pow(hbar*omega*p_m,2)/(E_p-
    SpeedOfLight*p_p*cos(Theta_p))*(E_m*(2*pow(tri_2
    ,2)*(pow(tri_2 ,2)-pow(tri_1 ,2))+8*pow(p_p*p_m*
```

```
     sin(Theta_p),2)*(pow(tri_2,2)+pow(tri_1,2)))+p_m
     *SpeedOfLight*(2*tri_1*tri_2*(pow(tri_2,2)-pow(
     tri_1,2))-tri_1*tri_2*pow(4*p_p*p_m*sin(Theta_p)
     ,2)))/(pow(tri_2,2)+pow(2*p_p*p_m*sin(Theta_p)
     ,2))+2*pow(hbar*omega*p_p*sin(Theta_p),2)*(2*
     tri_1*tri_2*p_m*SpeedOfLight+2*pow(tri_2,2)*E_m
     +8*pow(p_p*p_m*sin(Theta_p),2)*E_m)/(E_p-p_p*
     SpeedOfLight*cos(Theta_p))-2*pow(E_p*p_m,2)*(2*(
     pow(tri_2,2)-pow(tri_1,2))*pow(tri_2*E_m+tri_1*
     p_m*SpeedOfLight,2)+8*pow(p_p*p_m*sin(Theta_p)
     ,2)*((pow(tri_1,2)+pow(tri_2,2))*(pow(E_m,2)+pow
     (p_m*SpeedOfLight,2))+4*tri_1*tri_2*E_m*p_m*
     SpeedOfLight))/(pow(tri_2*E_m+tri_1*p_m*
     SpeedOfLight,2)+pow(2*rest_energy*p_p*p_m*sin(
     Theta_p),2))-8*pow(p_p*p_m*sin(Theta_p),2)*(pow(
     E_p,2)+pow(E_m,2))*(tri_2*p_m*SpeedOfLight+tri_1
     *E_m)/(E_p-SpeedOfLight*p_p*cos(Theta_p)));
  I[5]=-16*PI*pow(E_m,2)*pow(p_p,2)*pow(sin(Theta_p)
     ,2)*A/(pow(E_p-SpeedOfLight*p_p*cos(Theta_p),2)
     *(-pow(tri_2,2)+pow(tri_1,2)-4*pow(p_p,2)*pow(
     p_m,2)*pow(sin(Theta_p),2)));
}
else
{
  if (Theta_p!=PI)      // calculate cross section for
     0 degree
  {
    I[0]=2*B*p_m*SpeedOfLight/(tri_2*E_m+tri_1*p_m*
       SpeedOfLight);
    I[1]=-B*pow(p_m*SpeedOfLight,2)*(-pow(tri_1,2)+
       pow(tri_2,2))/(tri_2*pow(tri_2*E_m+tri_1*p_m*
       SpeedOfLight,2))*log((tri_1+tri_2)/(tri_1-
       tri_2));
    I[2]=-B*(2*tri_1*E_m*p_m*SpeedOfLight+tri_2*(pow(
       E_m,2)+pow(p_m*SpeedOfLight,2)))/(pow(tri_2*
       E_m+tri_1*p_m*SpeedOfLight,2))*log((E_m+p_m*
       SpeedOfLight)/(E_m-p_m*SpeedOfLight));
  I[3]=B*pow((4*E_p*p_m)/(tri_2*E_m+tri_1*p_m*
      SpeedOfLight),2);
  I[4]=8*B*pow(E_p*p_m,2)*(tri_1*E_m+tri_2*p_m*
      SpeedOfLight)/(pow(tri_2*E_m+tri_1*p_m*
      SpeedOfLight,3))*log(((tri_1-tri_2)*(E_m-p_m*
      SpeedOfLight))/((tri_1+tri_2)*(E_m+p_m*
      SpeedOfLight)));
  I[5]=-B*pow(2*hbar*p_m*omega,2)/(((tri_2*E_m+tri_1
      *p_m*SpeedOfLight)*(E_p-p_p*SpeedOfLight)*
      tri_2);
  I[6]=2*B*pow(hbar*p_m*omega,2)*(2*tri_1*tri_2*E_m
      +p_m*SpeedOfLight*(pow(tri_1,2)+pow(tri_2,2)))
      /(pow(tri_2*E_m+tri_1*p_m*SpeedOfLight,2)*(E_p
      -p_p*SpeedOfLight)*pow(tri_2,2))*log((tri_1+
      tri_2)/(tri_1-tri_2));
  I[7]=2*B*pow(hbar*omega,2)*p_m*(pow(E_m,2)-pow(
      p_m*SpeedOfLight,2))/(pow(tri_2*E_m+tri_1*p_m*
      SpeedOfLight,2)*(E_p-SpeedOfLight*p_p)*
      SpeedOfLight)*log((E_m-p_m*SpeedOfLight)/(E_m+
      p_m*SpeedOfLight));
}
else          // calculate cross section for 180
   degree
{
  I[0]=2*B*p_m*SpeedOfLight/(tri_2*E_m+tri_1*p_m*
      SpeedOfLight);
  I[1]=-B*pow(p_m*SpeedOfLight,2)*(-pow(tri_1,2)+
      pow(tri_2,2))/(tri_2*pow(tri_2*E_m+tri_1*p_m*
      SpeedOfLight,2))*log((tri_1+tri_2)/(tri_1-
      tri_2));
  I[2]=-B*(2*tri_1*E_m*p_m*SpeedOfLight+tri_2*(pow(
      E_m,2)+pow(p_m*SpeedOfLight,2)))/(pow(tri_2*
      E_m+tri_1*p_m*SpeedOfLight,2))*log((E_m+p_m*
      SpeedOfLight)/(E_m-p_m*SpeedOfLight));
  I[3]=B*pow((4*E_p*p_m)/(tri_2*E_m+tri_1*p_m*
      SpeedOfLight),2);
  I[4]=8*B*pow(E_p*p_m,2)*(tri_1*E_m+tri_2*p_m*
      SpeedOfLight)/(pow(tri_2*E_m+tri_1*p_m*
         SpeedOfLight,3))*log(((tri_1-tri_2)*(E_m-p_m*
         SpeedOfLight))/((tri_1+tri_2)*(E_m+p_m*
         SpeedOfLight)));
      I[5]=-B*pow(2*hbar*p_m*omega,2)/((tri_2*E_m+tri_1
         *p_m*SpeedOfLight)*(E_p+p_p*SpeedOfLight)*
         tri_2);
      I[6]=2*B*pow(hbar*p_m*omega,2)*(2*tri_1*tri_2*E_m
         +p_m*SpeedOfLight*(pow(tri_1,2)+pow(tri_2,2)))
         /(pow(tri_2*E_m+tri_1*p_m*SpeedOfLight,2)*(E_p
         +p_p*SpeedOfLight)*pow(tri_2,2))*log((tri_1+
         tri_2)/(tri_1-tri_2));
      I[7]=2*B*pow(hbar*omega,2)*p_m*(pow(E_m,2)-pow(
         p_m*SpeedOfLight,2))/(pow(tri_2*E_m+tri_1*p_m*
         SpeedOfLight,2)*(E_p+SpeedOfLight*p_p)*
         SpeedOfLight)*log((E_m-p_m*SpeedOfLight)/(E_m+
         p_m*SpeedOfLight));
    }
  }


  // sum up all terms to get value for cross section
  for (i=0;i<=7;i++)
  {
    cross=cross+I[i];
  }

  return cross; // give back result of cross section
     calculation
}
```

References

S. Agostinelli et al., 2003. G4-a simulation toolkit. Nucl. Instrum. Methods Phys. Res., Sect. A, vol. 506, pp. 250-303

H. Aiginger, 1966. Elektron-Bremsstrahlungwirkungsquerschnitte von 180 und 380 keV-Elektronen. Zeitschrift fuer Physik , vol. 197, pp. 8-25

L. P. Babich, 2003. High-energy phenomena in electric discharges in dense gases. Theory, experiment and natural phenomena. ISTC Science and technology series, vol. 2 Futurepast

H. A. Bethe and W. Heitler, 1934. On the stopping of fast particles and on the creaion of positive electrons. Proc. Phys. Soc. London, vol. 146, pp. 83-112

M. Briggs et al., 2010. First results on terrestrial gamma ray flashes from the Fermi Gamma-ray Burst Monitor. J. Geophys. Res., vol. 115, A07323

M. S. Briggs et al., 2011. Electron-positron beams from terrestrial lightning observed with Fermi GBM. Geophys. Res. Lett., vol. 38, L02808

B. E. Carlson, N. G. Lehtinen and U. S. Inan, 2009. Terrestrial gamma ray flashes production by lightning current pulses. J. Geophys. Res., vol. 114, A00E08

B. E. Carlson, N. G. Lehtinen and U. S. Inan, 2010. Terrestrial gamma ray flash production by active lightning leader channels. J. Geophys. Res., vol. 115, A10324

O. Chanrion and T. Neubert, 2008. A PIC-MCC code for simulation of streamer propagation in air. J. Comput. Phys., vol. 227, pp. 7222-7245

O. Chanrion and T. Neubert, 2010. Production of runaway electrons by negative streamer discharges. J. Geophys. Res., vol. 115, A00E32

D.E. Cullen, S.T. Perkins and S.M. Seltzer, 1991. Tables and Graphs of Electron Interaction Cross 10 eV to 100 GeV Derived from the LLNL Evaluated Electron Data Library (EEDL), Z = 1 - 100. Lawrence Livermore National Laboratory, UCRL-50400, vol. 31

S. A. Cummer, Y. Zhai, W. Hu, D. M. Smith, L. I. Lopez, M. A. Stanley, 2005. Measurements and implications of the relationship between lightning and terrestrial gamma ray flashes. Geophys. Res. Lett., vol. 32, L08811

J. R. Dwyer, 2003. A fundamental limit on electric fields in air. Geophys. Res. Lett., vol. 30, no. 2055

J. R. Dwyer and D. M. Smith, 2005. A comparison between Monte Carlo simulations of runaway breakdown and terrestrial gamma-ray flashes. Geophys. Res. Lett., vol. 32, L22804

J. R. Dwyer et al., 2005a. X-ray bursts associated with leader steps in cloud-to-ground lightning. Geophys. Res. Lett., vol. 32, L01803

J. R. Dwyer et al., 2005b. X-ray bursts produced by laboratory sparks in air. Geophys. Res. Lett., vol. 32, L20809

J. R. Dwyer, 2007. Relativistic breakdown in planetary atmospheres, Physics of plasmas. vol. 14, no. 042901

J. R. Dwyer et al., 2008a. A study of X-ray emission from laboratory sparks in air at atmospheric pressure. J. Geophys. Res., vol. 113, D23207

J. R. Dwyer et al., 2008b. High-energy electron beams launched into space by thunderstorms. Geophys. Res. Lett., vol. 35, L02815

G. Elwert and E. Haug, 1969. Calculation of Bremsstrahlung cross sections with Sommerfeld-Maue eigenfunctions. Phys. Rev., vol. 183, pp. 90-105

J. K. Fink and R. H. Pratt, 1973. Use of Furry-Sommerfeld-Maue wave functions in pair production and Bremsstrahlung. Phys. Rev. A, vol. 7, pp. 392-403

G. J. Fishman et al., 1994. Discovery of intense gamma-ray flashes of atmospheric origin. Science, vol. 264, pp. 1313-1316

I. Gallimberti et al., 2002. Fundamental processes in long air gap discharges. C. R. Physique, vol. 3, pp. 1335-1359

T. Gjesteland, N. Ostgaard, A.B. Collier, B.E. Carlson, M.B. Cohen, N.G. Lehtinen, 2011. Confining the angular distribution of terrestrial-gamma ray flash emission. J. Geophys. Res., vol. 116, A11313

B. W. Grefenstette, D. M. smith, B. J. Hazelton and L. I. Lopez, 2009. First RHESSI terrestrial gamma ray flash catalog. J. Geophys. Res., vol. 114, A02314

W. Greiner and J. Reinhardt, 1995. Quantenelektrodynamik, Verlag Harri Deutsch

A. V. Gurevich, 1961. On the theory of runaway electrons. Soviet Physics Jetp-USSR, vol. 12, pp. 904-912

A. V. Gurevich, G. Milikh, R. Roussel-Dupré, 1992. Runaway electron mechanism of air breakdown and preconditioning during a thunderstorm. Phys. Lett. A, vol. 165, pp. 463-468

A. V. Gurevich and K. P. Zybin, 2001. Runaway breakdown and electric discharges in thunderstorms. Physics-Uspekhi, vol. 44, pp. 1119-1140

W. Heitler, 1944. The quantum theory of radiation. Oxford University Press

P.V.C. Hough, 1948. The angular distribution of pair-produced electrons and Bremsstrahlung. Phys. Rev., vol. 74, pp. 80-86

U. S. Inan and N. G. Lehtinen, 2005. Production of terrestrial gamma-ray flashes by an electromagnetic pulse from a lightning return stroke. Geophys. Res. Lett., vol. 32, L19818

J. D. Jackson, 1975. Classical electrodynamics. John Wiley & Sons

H. W. Koch and J. W. Motz, 1959. Bremsstrahlung Cross-Section Formulas and Related Data. Rev. Mod. Phys., vol. 31, pp. 920-956

I. D. Kostyrya, V. F. Tarasenko, A. N. Tkachev and S. I. Yakovlenko, 2006. X-ray radiation due to nanosecond volume discharges in air under atmospheric pressure. Techn. Phys., vol. 51, pp. 356-361

N.G. Lehtinen, 2000. Relativistic runaway electrons above thunderstorms. Ph.D. thesis, Stanford University, Stanford, CA

C. Li, W. J. M. Brok, U. Ebert and J. J. A. M. van der Mullen, 2007. Deviations from the local field approximation in negative streamer heads. J. Appl. Phys., vol. 101, no. 123305

C. Li, U. Ebert and W. Hundsdorfer, 2009. 3D hybrid computations for streamer discharges and production of runaway electrons. J. Phys. D-Appl. Phys., vol. 42, no. 202003

C. Li, U. Ebert and W. Hundsdorfer, 2010. Spatially hybrid computations for streamer discharges with generic features of pulled fronts: I. Planar fronts. J. Comput. Phys., vol. 229, pp. 200-220

G. Lu, S. A. Cummer, J. Li, F. Han, D. M. Smith and B. Grefenstette, 2011. Characteristics of broadband magnetic lightning emissions associated with terrestrial gamma-ray flashes. J. Geophys. Res., vol. 116, A03316

V. March and J. Montanyà, 2010. Influence of the voltage-time derivative in X-ray emission from laboratory sparks. Geophys. Res. Lett., vol. 37, L19801

M. Marisaldi et. al., 2010. Detection of terrestrial gamma ray flashes up to 40 MeV by the AGILE satellite. J. Geophys. Res., vol. 115, A00E13

G. Milikh and R. Roussel-Dupré, 2010. Runaway breakdown and electrical discharges in thunderstorms. J. Geophys. Res., vol. 115, A00E60

C. B. Moore, K. B. Eack, G. D. Aulich and W. Rison, 2001. Energetic radiation associated with lightning stepped-leaders. Geophys. Res. Lett., vol. 28, pp. 2141-2144

G. D. Moss, V. P. Pasko, N. Y. Liu and G. Veronis, 2006. Monte Carlo model for analysis of thermal runaway electrons in streamer tips in transient luminous events and streamer zones of lightning leaders. J. Geophys. Res., vol. 111, A02307

W. Nackel, 1994. The elementary process of Bremsstrahlung. Phys. Rep., vol. 243, pp. 317-353

C. V. Nguyen, A. P. J. van Deursen and Ute Ebert, 2008. Multiple x-ray bursts from long discharges in air. J. Phys. D-Appl. Phys., vol. 41, no. 234012

C. V. Nguyen, A. P. J. van Deursen E. J. M. van Heesch and G. J. J. Winands, 2010. X-ray emission in streamer-corona plasma. J. Phys. D-Appl. Phys., vol. 43, no. 025202

P. E. Penczynski and H. L. Wehner, 1970. Measurement of the energetic and angular dependence of the external Bremsstrahlung asymmetry. Z. Physik, vol. 237, pp. 75-85

M. E. Peskin and D. V. Schroeder, 1995. An introduction to quantum field theory, Westview Press

A. V. Phelps, B. M. Jelenkovic and L. C. Pitchford, 1987. Simplified models of electron excitation and ionizattion at very high E/n. Phys. Rev. A, vol. 36, no. 5327

M. Rahman, V. Cooray, N. A. Ahmad, J. Nyberg, V. A. Rakov and S. Sharma, 2008. X-rays from 80 cm long sparks in air. Geophys. Res. Lett., vol. 35, L06805

A. G. Rep'ev and P. B. Repin, 2008. Spatiotemporal parameters of the X-ray radiation from a diffuse atmospheric-pressure discharge. Techn. Phys., vol. 53, pp. 73-80

S.M.Seltzer and M.J.Berger, 1985. Bremsstrahlung spectra from electron interactions with screened atomic nuclei and orbital electrons. Nucl. Inst. Meth. B12, pp. 95-134

C. D. Shaffer, X. M. Tong and R. H. Pratt, 1996. Triply differential cross section and polarization correlations in electron Bremsstrahlung emission. Phys. Rev. A, vol. 53, pp. 4158-4163

C. D. Shaffer and R. H. Pratt, 1997. Comparison of relativistic partial-wave calculations of triply differential electron-atom bremsstrahlung with simpler theories. Phys. Rev. A, vol. 56, pp. 3653-3658

T. Shao, C. Zhang, Z. Niu, P. Yan, V. F. Tarasenko, E. K. Baksht, A. G. Burahenko and Y. B. Shut'ko, 2011. Diffuse discharge, runaway electron, and x-ray in atmospheric pressure air in a inhomogeneous electrical field in repetitive pulsed modes. Appl. Phys. Lett., vol. 98, no. 021506

D. M. Smith, L. I. Lopez, R. P. Lin and C. P. Barrington-Leigh, 2005. Terrestrial gamma-ray flashes observed up to 20 Mev. Science, vol. 307, pp. 1085-1088

D. M. Smith et al., 2010. Terrestrial gamma ray flashes correlated to storm phase and tropopause height. J. Geophys. Res., vol. 115, A00E49

D. M. Smith, J. Dwyer, B. Hazelton, B. Greffenstette, G. F. M. Martinez-McKinney, Z. Zhang, A. Lowell, N. Kelley, M. Splitt, S. Lazarus, W. Ulrich, M. Schaal, Z. Saleh, E. Cramer, H. Rassoul, S.A. Cummer, G. Lu and R. Blakeslee, 2011. The rarity of terrestrial gamma-ray flashes. Geophys. Res. Lett., vol. 38, L08807

Y. L. Stankevich and V. G. Kalinin, 1967. Fast electrons and X-ray radiation during the initial stage of growth of a pulsed spark discharge in air. Sov. Phys. Dokl., vol. 12, pp. 1042-1043

M. Tavani et al., 2011. Terrestrial gamma-ray flashes as powerful particle accelerators. Phys. Rev. Lett., vol. 106, no. 018501

T. Torii, T. Nishijima, Zl. Kawasaki, T. Sugita, 2004. Downward emission of runaway electrons and bremsstrahlung photons in thunderstorm electric fields. Geophys. Res. Lett., vol. 31, L05113

Y-S. Tsai, 1974. Rev. Mod. Phys, vol. 46, p. 815

Y-S. Tsai, 1977. Rev. Mod. Phys, vol. 49, p. 421

H. K. Tseng and R. H. Pratt, 1971. Exact screened calculations of atomic-field Bremsstrahlung. Phys. Rev. A, vol. 3, pp. 100-115

H. Tsuchiya, T. Enoto, S. Yamada, T. Yuasa, K. Nakazawa, T. Kitaguchi, M. Kawaharada, M. Kokubun, H. Kato, M. Okano, K. Makishima, 2011. Long-duration gamma ray emissions from 2007 and 2008 winter thunderstorms. J. Geophys. Res., vol. 116, D09113

C. Wilson, 1925. The electric field of a thundercloud and some of its effects. Proc. Phys. Soc. London, vol. 37A, pp. 32D-37D

Vitae:

Christoph Köhn studied physics in Kiel and Hamburg, Germany from 2005 till 2010. After having finished his diploma thesis on six-dimensional supergravity, he started his PhD studies at CWI Amsterdam, The Netherlands.

Ute Ebert studied physics at the University of Heidelberg, Germany, and she wrote her PhD thesis at the University of Essen, Germany. After a postdoc period at the University of Leiden, Netherlands, she became staff member at CWI Amsterdam, Netherlands. Since 2002 she leads a research group at CWI and is part time professor at Eindhoven University of Technology. The research of her group concentrates on transient electrical discharges, both in plasma technology and in atmospheric electricity.

- Analytical results on doubly differential cross-sections for typical TGF parameters
- Distribution of emission angles and energies for Bremsstrahlung photons
- Distribution of emission angles and energies for positrons in pair production
- C++ code with the analytical cross section results provided